Copy 419
RM L57A30a

NACA

RESEARCH MEMORANDUM

THEORETICAL INVESTIGATION OF THE EFFECT OF RUDDER AND STABILIZER DEFLECTIONS ON THE ANGLES OF ATTACK AND SIDESLIP IN RAPID ROLLS

By C. H. Woodling

Langley Aeronautical Laboratory
Langley Field, Va.

NATIONAL ADVISORY COMMITTEE FOR AERONAUTICS

WASHINGTON

March 27, 1957

NATIONAL ADVISORY COMMITTEE FOR AERONAUTICS

RESEARCH MEMORANDUM

THEORETICAL INVESTIGATION OF THE EFFECT OF RUDDER AND STABILIZER DEFLECTIONS ON THE ANGLES OF ATTACK AND SIDESLIP IN RAPID ROLLS

By C. H. Woodling

SUMMARY

A theoretical investigation has been made of the effects of rudder and stabilizer deflections on the angles of attack and sideslip experienced by an airplane in rapid rolls. Expressions are derived from the five-degree-of-freedom airplane equations of motion which define the rudder and stabilizer motions necessary to maintain constant angle of attack and zero sideslip during an aileron roll. These expressions are simplified and considered as the basis for automatic controls. The effect on the rolling behavior of the airplane of applying ramp-type rudder and stabilizer deflections, similar to the exact rudder and stabilizer inputs in magnitude and direction, is also investigated. The results are presented, for the most part, as time histories of the airplane response to aileron deflections with and without rudder and stabilizer inputs. Maximum loads experienced by the vertical and horizontal tail surfaces during aileron rolls are calculated for the automatic control investigation.

The control motions calculated by using the expressions which are derived from the airplane equations of motion are useful in determining the magnitude and direction of the rudder and stabilizer deflections that might be applied by a pilot or by automatic controls to maintain small angles of attack and sideslip variations in aileron rolls. For the airplane configuration and flight condition investigated, the ramp-type rudder and stabilizer deflections were effective in reducing the angles of attack and sideslip in rapid rolls. The automatic rudder and stabilizer had a large favorable effect on the rolling behavior of the airplane for the cases investigated. The maximum loads on the vertical and horizontal tail surfaces were generally reduced when the automatic controls were applied.

INTRODUCTION

Current fighter airplanes have experienced large changes in angles of attack and sideslip, resulting in excessive loads, during rapid rolling maneuvers. A simplified linear analysis of the problem reported in references 1 and 2 indicated that roll coupling between the lateral and longitudinal modes could cause an instability in the form of a divergent motion as the rolling velocity of the airplane approaches the natural frequency of the airplane in yaw or pitch. The design trend of fighter airplanes resulting in large inertia about the pitch and yaw axes relative to that about the roll axis, coupled with the loss in directional stability as Mach number increases, are predominant factors contributing to the aforementioned uncontrollable motions.

Theoretical studies of various means of reducing roll coupling have been made in references 3, 4, and 5. References 3 and 4 pointed out that increased pitch damping was very effective in reducing the angles of attack and sideslip obtained in aileron rolls. Reference 5 presented a method of avoiding roll-coupling instability in which rudder and stabilizer inputs were automatically applied to counteract the yawing and pitching moments produced on the rolling airplane by the predominant inertia coupling terms. This paper investigates the possibility of applying the rudder and stabilizer in coordination with the ailerons so as to roll the airplane with minimum variations in the angles of attack and sideslip. The analysis first determines the exact rudder and stabilizer inputs that would be required to roll an airplane with $\Delta\alpha$ and β identically equal to zero. By using these exact rudder and stabilizer inputs as an indication of the direction and approximate magnitude of the controls required, the effect of simple ramp-type deflections such as might be applied by a pilot are investigated. Finally the exact control expressions are simplified and considered as equations for automatic controls, and their effect on the rolling airplane are studied. Time histories of the controls and the time responses of the rolling airplane, calculated on an electronic analog computer, are presented. Since the loads on the horizontal and vertical tails are dependent on the magnitude of the rudder and stabilizer deflections, as well as the motions of the airplane, the maximum loads with and without the automatic rudder and stabilizer are computed and compared.

The rudder and stabilizer expressions defining the controls required for rolling at constant angle of attack and zero sideslip are derived from the five-degree-of-freedom airplane equation of motion. The quantitative results, such as the airplane time histories and the tail loads calculations, are for a swept-wing airplane configuration flying at one altitude and Mach number.

SYMBOLS

The forces and moments are referred to the body axes system shown in figure 1.

L rolling moment, ft-lb

M pitching moment, ft-lb

N yawing moment, ft-lb

Y side force, lb

C_L lift coefficient, $\frac{\text{Lift}}{\frac{1}{2}\rho V^2 S}$

C_Y lateral-force coefficient, $\frac{Y}{\frac{1}{2}\rho V^2 S}$

C_l rolling-moment coefficient, $\frac{L}{\frac{1}{2}\rho V^2 Sb}$

C_m pitching-moment coefficient, $\frac{M}{\frac{1}{2}\rho V^2 S\bar{c}}$

C_n yawing-moment coefficient, $\frac{N}{\frac{1}{2}\rho V^2 Sb}$

$C_{l_{\delta_a}}$ rate of change of rolling-moment coefficient with aileron deflection, per radian

$C_{n_{\delta_r}}$ rate of change of yawing-moment coefficient with rudder deflection, per radian

$C_{n_{\delta_a}}$ rate of change of yawing-moment coefficient with aileron deflection, per radian

$C_{m_{i_t}}$ rate of change of pitching moment with stabilizer deflection (horizontal tail), per radian

δ_a	total aileron deflection, radians unless otherwise noted
i_t	stabilizer deflection, positive when trailing edge is down, radians unless otherwise noted
Δi_t	stabilizer deflection from trim value, deg
δ_r	rudder deflection, positive when trailing edge is to the left, radians unless otherwise noted
S	wing area, sq ft
b	wing span, ft
$\bar{c}$	mean aerodynamic chord, ft
ρ	air density, slugs/cu ft
V	velocity, ft/sec
ϵ	angle between body axis and principal X-axis, positive when reference axis is above principal axis at the nose, deg
I_X, I_Y, I_Z	moments of inertia about X, Y, and Z body axes, respectively, slug-ft^2
I_{XZ}	product of inertia (positive when principal axis is inclined below X-body axis), slug-ft^2
I_{X_e}	moment of inertia of rotating engine parts about X-body axis, slug-ft^2
m	mass of airplane, W/g, slugs
W	weight of airplane, lb
g	acceleration due to gravity, 32.2 ft/sec^2
n_g	normal lift acceleration at center of gravity, g units
α	angle of attack of airplane body axis, radians unless otherwise noted
$\Delta\alpha$	change in angle of attack from initial or trim value, deg
β	angle of sideslip, radians unless otherwise noted

ϕ angle of roll, radians

ψ angle of yaw, radians

p rolling angular velocity, radians/sec

q pitching angular velocity, radians/sec

r yawing angular velocity, radians/sec

ω_e engine rotational velocity, radians/sec

l_3,m_3,n_3 direction cosines describing orientation of airplane axis system (see ref. 3)

t time, sec

$$C_{L_\alpha} = \frac{\partial C_L}{\partial \alpha}$$

$$C_{m_\alpha} = \frac{\partial C_m}{\partial \alpha}$$

$$C_{m_q} = \frac{\partial C_m}{\partial \frac{q\bar{c}}{2V}}$$

$$C_{m_{\dot{\alpha}}} = \frac{\partial C_m}{\partial \frac{\dot{\alpha}\bar{c}}{2V}}$$

$$C_{l_\beta} = \frac{\partial C_l}{\partial \beta}$$

$$C_{n_\beta} = \frac{\partial C_n}{\partial \beta}$$

$$C_{Y_\beta} = \frac{\partial C_Y}{\partial \beta}$$

$$C_{l_p} = \frac{\partial C_l}{\partial \frac{pb}{2V}}$$

$$C_{l_r} = \frac{\partial C_l}{\partial \frac{rb}{2V}}$$

$$C_{n_p} = \frac{\partial C_n}{\partial \frac{pb}{2V}}$$

$$C_{n_r} = \frac{\partial C_n}{\partial \frac{rb}{2V}}$$

$$L_{\delta_a} = \frac{\rho V^2 Sb}{2} C_{l_{\delta_a}}$$

$$L_p = \frac{\rho V S b^2}{4} C_{l_p}$$

$$L_r = \frac{\rho V S b^2}{4} C_{l_r}$$

$$L_\beta = \frac{\rho V^2 Sb}{2} C_{l_\beta}$$

$$N_{\delta_r} = \frac{\rho V^2 Sb}{2} C_{n_{\delta_r}}$$

$$N_{\delta_a} = \frac{\rho V^2 Sb}{2} C_{n_{\delta_a}}$$

$$N_r = \frac{\rho V S b^2}{4} C_{n_r}$$

$$N_p = \frac{\rho V S b^2}{4} C_{n_p}$$

$$N_\beta = \frac{\rho V^2 Sb}{2} C_{n_\beta}$$

$$Y_\beta = \frac{\rho V^2 S}{2} C_{Y_\beta}$$

$$M_{i_t} = \frac{\rho V^2 S\bar{c}}{2} C_{m_{i_t}}$$

$$M_q = \frac{\rho V S\bar{c}^2}{4} C_{m_q}$$

$$M_{\dot{\alpha}} = \frac{\rho V S\bar{c}^2}{4} C_{m_{\dot{\alpha}}}$$

$$M_\alpha = \frac{\rho V^2 S\bar{c}}{2} C_{m_\alpha}$$

$$L'_\alpha = \frac{\rho V^2 S}{2} C_{L_\alpha}$$

Subscript:

o initial condition

cg center of gravity

A dot over a symbol represents a derivative with respect to time.

EQUATIONS OF MOTION

The nonlinear airplane equations of motion, referred to airplane body axes (fig. 1) and assuming constant forward speed, may be written as follows:

Rolling-moment equation

$$\dot{p} = \frac{I_Y - I_Z}{I_X} qr + \frac{I_{XZ}}{I_X} (\dot{r} + pq) + \frac{L_{\delta_a}}{I_X} \delta_a + \frac{L_p}{I_X} p + \frac{L_r}{I_X} r + \frac{L_\beta}{I_X} \beta$$

Pitching-moment equation

$$\dot{q} = \frac{I_Z - I_X}{I_Y} pr + \frac{I_{XZ}}{I_Y} (r^2 - p^2) - \frac{I_{X_e}\omega_e}{I_Y} r + \frac{M_{i_t}}{I_Y} i_t + \frac{M_q}{I_Y} q + \frac{M_{\dot{\alpha}}}{I_Y} \dot{\alpha} + \frac{M_\alpha}{I_Y} \alpha$$

Yawing-moment equation

$$\dot{r} = \frac{I_X - I_Y}{I_Z} pq + \frac{I_{XZ}}{I_Z} (\dot{p} - qr) + \frac{I_{X_e} \omega_e}{I_Z} q + \frac{N_{\delta_r}}{I_Z} \delta_r + \frac{N_{\delta_a}}{I_Z} \delta_a + \frac{N_r}{I_Z} r + \frac{N_p}{I_Z} p + \frac{N_\beta}{I_Z} \beta$$

Lateral-force equation

$$\dot{\beta} = \alpha p - r + \frac{g}{V} m_3 + \frac{Y_\beta}{mV} \beta$$

Normal-force equation

$$\dot{\alpha} = q - p\beta + \frac{g}{V} n_3 - \frac{L'_\alpha}{mV} \alpha$$

Direction cosine equations

$$\dot{l}_3 = m_3 r - n_3 q$$

$$\dot{m}_3 = n_3 p - l_3 r$$

$$\dot{n}_3 = l_3 q - m_3 p$$

The direction cosine equations were used to include the proper component of the gravity vector in the two force equations.

ANALYSIS

This paper investigates the possibility of applying rudder and stabilizer, either by a pilot or by an automatic control, in coordination with the ailerons so as to roll the airplane with a minimum of variation in the angles of attack and sideslip. The analysis determines the exact rudder and stabilizer motions that are required to roll an airplane with $\Delta\alpha$ and β identically equal to zero. Based on these control motions an indication is obtained of the direction and magnitude of rudder and stabilizer that might be applied by a pilot to maintain small variations in the angles of attack and sideslip during rapid rolls. The exact rudder and stabilizer expressions are simplified and considered as possible automatic controls equations.

Rudder and Stabilizer Required for Zero Variation of the Angles of Attack and Sideslip

First, consider the lateral- and normal-force equations for $\Delta\alpha = \beta = \dot{\alpha} = \dot{\beta} = 0$. If it is assumed that the rolling is initiated from $\alpha = \alpha_o$, the lateral-force equation becomes

$$0 = \alpha_o p - r + \frac{g}{V} m_3 \tag{1}$$

and the normal-force equation becomes

$$0 = q + \frac{g}{V} n_3 - \frac{L'_\alpha}{mV} \alpha_o \tag{2}$$

From equation (1) the yaw rate is

$$r = \alpha_o p + \frac{g}{V} m_3 \tag{3}$$

and the time rate of change of r is

$$\dot{r} = \alpha_o \dot{p} + \frac{g}{V} \dot{m}_3 \tag{3a}$$

From equation (2) the pitch rate is

$$q = \frac{L'_\alpha}{mV} \alpha_o - \frac{g}{V} n_3 \tag{4}$$

and the time rate of change of q is

$$\dot{q} = -\frac{g}{V} \dot{n}_3 \tag{4a}$$

Thus, if the rudder and stabilizer are applied during the rolling maneuver so as to produce the yaw rate and yaw acceleration as prescribed by equations (3) and (3a) and the pitch rate and pitch acceleration as prescribed by equations (4) and (4a), the angle of attack and angle of sideslip will be zero according to the lateral- and normal-force equations.

The rudder required to produce the prescribed velocities and accelerations is obtained by substituting for r, $\dot{r}$, q, and $\dot{q}$, equations (3), (3a), (4), and (4a) into the yawing-moment equation and also remembering that $\Delta\alpha$ and β are assumed zero. This substitution yields

$$\delta_r = \frac{I_Z}{N_{\delta_r}}\left\{\left(\alpha_o - \frac{I_{XZ}}{I_Z}\right)\dot{p} - \left[\left(\frac{I_X - I_Y}{I_Z}\right)\frac{L'_\alpha}{mV}\alpha_o - \frac{I_{XZ}}{I_Z}\frac{L'_\alpha}{mV}\alpha_o^2 + \right.\right.$$

$$\left.\frac{N_r}{I_Z}\alpha_o + \frac{N_p}{I_Z}\right]p + \left(\frac{g}{V}\right)\left[\left(\frac{I_X - I_Y}{I_Z}\right) - \frac{I_{XZ}}{I_Z}\alpha_o\right]n_3 p + \left(\frac{g}{V}\right)\dot{m}_3 +$$

$$\left(\frac{g}{V}\right)\left(\frac{I_{XZ}}{I_Z}\frac{L'_\alpha}{mV}\alpha_o - \frac{N_r}{I_Z}\right)m_3 + \left(\frac{g}{V}\right)\left(\frac{I_{X_e}\omega_e}{I_Z}\right)n_3 - \left(\frac{g}{V}\right)^2\left(\frac{I_{XZ}}{I_Z}\right)n_3 m_3 -$$

$$\left.\left(\frac{I_{X_e}\omega_e}{I_Z}\frac{L'_\alpha}{mV}\alpha_o\right) - \frac{N_{\delta_a}}{I_Z}\delta_a\right\} \tag{5}$$

The stabilizer required to produce the prescribed velocities and accelerations is obtained by making the same substitutions into the pitching-moment equation. Thus,

$$i_t = \frac{I_Y}{M_{i_t}}\left\{-\left[\left(\frac{I_Z - I_X}{I_Y}\right)\alpha_o + \frac{I_{XZ}}{I_Y}\left(\alpha_o^2 - 1\right)\right]p^2 + \left(\frac{I_{X_e}\omega_e}{I_Y}\alpha_o\right)p - \right.$$

$$\left(\frac{g}{V}\right)\left[\left(\frac{I_Z - I_X}{I_Y}\right) + 2\alpha_o\frac{I_{XZ}}{I_Y}\right]m_3 p - \left(\frac{g}{V}\right)\dot{n}_3 + \left(\frac{g}{V}\right)\left(\frac{I_{X_e}\omega_e}{I_Y}\right)m_3 -$$

$$\left.\left(\frac{g}{V}\right)^2\left(\frac{I_{XZ}}{I_Y}\right)m_3^2 + \left(\frac{g}{V}\right)\left(\frac{M_q}{I_Y}\right)n_3 - \left(\frac{M_q}{I_Y}\frac{L'_\alpha}{mV}\alpha_o\right) - \left(\frac{M_\alpha}{I_Y}\alpha_o\right)\right\} \tag{6}$$

From expressions (5) and (6), therefore, one can determine, for a particular airplane and flight condition, the ideal rudder and stabilizer motions required for $\Delta\alpha = \beta = 0$ in a rolling maneuver. These inputs (as given by eqs. (5) and (6)) will hereafter be referred to as the exact control inputs. They are exact in the sense that they will produce $\Delta\alpha$ and β identically equal to zero for any rolling input according to the equations from which they were derived.

Automatic Rudder and Stabilizer Deflections for $\Delta\alpha$ and β Approximately Equal to Zero

The expressions for the proposed automatic controls are derived from the exact control equations. In order to simplify the exact rudder and stabilizer expressions (eqs. (5) and (6)), it is assumed that they are derived from the equations of motion referenced to principal body axes. In practice if the sensing instruments for the automatic controls are alined to record the motions of the airplane relative to the principal body axes then the effect of the product of inertia on the recorded quantities will be zero. Therefore the I_{XZ} terms in expressions (5) and (6) are zero. The angle of attack in equations (5) and (6) now is the angle of attack of the principal X-axis of the airplane. Also the assumption is made that the gravity terms in equations (3) and (4) can be neglected. The terms $\frac{g}{V} m_3$ and $\frac{g}{V} n_3$ contain the effect of the rotating gravity vector in the two force equations. During a rapid roll with small pitch rate, these vary approximately as $\sin pt$ and $\cos pt$, respectively. These terms are not necessarily small as compared with $\alpha_O p$ and $\frac{L'_\alpha}{mV} \alpha_O$. However, since m_3 and n_3 are approximately periodic, it is assumed that they can be neglected and that the desired yaw and pitch rates will be the mean values as determined by equations (3) and (4). That is

$$r = \alpha_O p \tag{7}$$

and

$$q = \frac{L'_\alpha}{mV} \alpha_O \tag{8}$$

Also from equation (7), $\dot{r}$ is

$$\dot{r} = \alpha_O \dot{p} \tag{9}$$

and from equation (8), $\dot{q}$ is

$$\dot{q} = 0 \tag{10}$$

Substitution of equations (7), (8), (9), and (10) into the yawing-moment and pitching-moment equations for $I_{XZ} = \Delta\alpha = \beta = 0$, which is equivalent to setting the I_{XZ} and gravity terms to zero in equations (5) and (6), yields

$$\delta_r = \frac{I_Z}{N_{\delta_r}}\left\{\alpha_o\dot{p} - \left[\left(\frac{I_X - I_Y}{I_Z}\right)\frac{L'_\alpha}{mV}\alpha_o + \frac{N_r}{I_Z}\alpha_o + \frac{N_p}{I_Z}\right]p - \frac{N_{\delta_a}}{I_Z}\delta_a - \frac{I_{X_e}\omega_e}{I_Z}\frac{L'_\alpha}{mV}\alpha_o\right\} \tag{11}$$

and

$$i_t = \frac{I_Y}{M_{i_t}}\left\{-\left[\left(\frac{I_Z - I_X}{I_Y}\right)\alpha_o\right]p^2 + \left(\frac{I_{X_e}\omega_e}{I_Y}\alpha_o\right)p - \left(\frac{M_q}{I_Y}\frac{L'_\alpha}{mV}\alpha_o + \frac{M_\alpha}{I_Y}\alpha_o\right)\right\} \tag{12}$$

If these controls are to operate only while the airplane is rolling, some further modifications can be made. The last term in equation (11) defines the rudder required to counteract the yawing moment on the airplane produced by the engine gyroscopic term $I_{X_e}\omega_e$ and the pitching velocity $q = \frac{L'_\alpha}{mV}\alpha_o$. If this term is retained in the rudder equation the yawing torque will be automatically compensated for. However in this analysis the term is deleted assuming that in a g maneuver if the yawing moment due to the engine is noticeable, the pilot will generally apply approximate corrective rudder. The last two terms or the stabilizer equation, which are not a function of the roll rate, are also deleted. These two terms define the approximate stabilizer deflection required to trim the airplane at α_o. If the gravity term $\frac{g}{V}n_3$ had not been neglected (in eq. (8)), in the derivation of the automatic control equations, the trim value of i_t would be determined exactly by these two terms. Assuming then that the pilot will apply the necessary stabilizer deflection to trim the airplane at α_o, the incremental stabilizer to be applied automatically during a rolling maneuver is given by the first two terms of equation (12). When those terms which have been suggested are deleted, the final equations to be used for the automatic rudder and stabilizer are as follows:

$$\delta_r = \frac{I_Z}{N_{\delta_r}}\left\{\alpha_o\dot{p} - \left[\left(\frac{I_X - I_Y}{I_Z}\right)\frac{L'_\alpha}{mV}\alpha_o + \frac{N_r}{I_Z}\alpha_o + \frac{N_p}{I_Z}\right]p - \frac{N_{\delta_a}}{I_Z}\delta_a\right\} \tag{13}$$

and

$$\Delta i_t = \frac{I_Y}{M_{i_t}} \left\{ - \left[\left(\frac{I_Z - I_X}{I_Y} \right) \alpha_o \right] p^2 + \left(\frac{I_{X_e} \omega_e}{I_Y} \alpha_o \right) p \right\} \tag{14}$$

The term α_o appearing in the stabilizer and rudder expressions is defined as the initial angle of attack or the angle of attack from which the roll is initiated. If the airplane is rolled from 2g or 3g flight, the α_o in the stabilizer and rudder expressions must be the α_o corresponding to 2g or 3g. It is of interest to note that expressions (7), (8), and (9) indicate that the larger the α_o (higher g conditions) from which the airplane is rolled, the higher the required yaw rate and acceleration (for the same roll rate) and the pitch rate must be. These higher rates result in proportionally larger required rudder and stabilizer deflections.

RESULTS AND DISCUSSION

The results of the analysis are for the most part presented as time histories of airplane motion and control inputs computed on an electronic analog computer. These results are divided into three parts, namely:

(1) Time histories of the exact rudder and stabilizer inputs calculated by equations (5) and (6) for several g conditions and several aileron deflections.

(2) Time histories of the airplane response in aileron rolls to ramp rudder and stabilizer inputs similar to the exact control inputs in magnitude and direction.

(3) The effect of automatic rudder and stabilizer control on the airplane response in aileron rolls and calculation of the vertical and horizontal tail loads produced by these controls during rolling.

The time histories were calculated using the five-degree-of-freedom airplane equations of motion. The airplane used in this study was a swept-wing fighter airplane configuration, assumed to be flying at an altitude of 32,000 feet and a Mach number of 0.7. The stability derivatives, mass characteristics of the airplane and other constants used in the study are presented in table I. All the time histories presented are for left rolls only, since for the conditions investigated this direction of roll is more severe than right rolls. This difference in right and left rolls can be attributed to the asymmetric moments produced on the aircraft by the rotating engine (refs. (3) and (6)). The analog runs

for rolls with aileron alone, that is, stabilizer and rudder not applied, are for approximately 360° roll angle. Generally, for these cases the airplane after rolling 360° would not remain at zero bank angle but would reverse in roll direction due to the rolling moment produced by the effective dihedral. No attempt was made to stop this rolling after the 360° roll angle was obtained. A simple ramp-type aileron input with a 50° per second rate was used throughout the investigation.

Exact Rudder and Stabilizer Inputs

for $\Delta\alpha = \beta = 0$

The airplane time histories with and without the exact rudder and stabilizer inputs and also the time histories of the rudder and stabilizer deflections calculated by equations (5) and (6) are shown in figure 2. The two cases on each figure are compared for the same aileron input. Figure 2(a) shows the response of the airplane to a 20° ramp aileron deflection. The airplane is initially at 1 g trim flight and rolled from this condition. For the aileron-alone case, i_t is held at its initial trim value and δ_r at zero. For this case the angle of attack and angle of sideslip reach values of -5° and -20°, respectively, during the rolling. Notice the rapid change experienced in the angles of attack and sideslip during the recovery phase, that is, after the aileron has been returned to zero. When δ_r and Δi_t are applied as defined by equations (5) and (6), respectively, the angle of attack remains at its initial value and the angle of sideslip remains at zero during the rolling. It should be noted that the roll rate response is somewhat improved. The lack of overshoot in the roll rate response during the recovery phase and the higher level of rolling velocity for zero $\Delta\alpha$ and β is mainly the result of zero dihedral effect during the maneuver. The increase in the roll velocity is more pronounced in some of the subsequent figures. The maximum incremental stabilizer deflection required is about +2°. It is interesting to note that the direction of the stabilizer is such to produce a pitch-down moment on the airplane, or probably opposite stabilizer to that which a pilot would instinctively apply as he experienced the negative normal g due to the angle of attack. The maximum rudder deflection required is about +14° and -5°. The change in sign of the rudder deflection is principally due to the $\dot{p}$ term in the δ_r equation (eq. (5)).

Figure 2(b) shows the response of the airplane to a 30° ramp aileron input. The airplane is initially at 1 g trim flight. For the aileron-alone case, the maximum excursions in α and β are slightly less than those shown in figure 2(a). According to reference 3, which presents an

analysis for an airplane of almost identical mass and aerodynamic characteristics and for the same flight condition, the maximum excursions in α and β due to roll coupling occur for average roll rates between -1.5 and -2.0 radians per second. Average roll rate in this case is defined as 2π divided by the time required to roll to 360°. Although the roll angle record is not shown for the cases presented in this paper, the average roll rate calculated from unpublished analog results for figure 2(a) is about -1.9 radians per second and for figure 2(b) about -2.4 radians per second. This explains the slight decrease in the maximum angles obtained for figure 2(b) as compared with figure 2(a). The maximum incremental stabilizer and the rudder deflections required for $\Delta\alpha = \beta = 0$ are larger than those for $\delta_a = 20^{\circ}$ due to the dependency of the i_t and δ_r on the roll rate. Comparison of figures 2(a) and 2(b) also indicates that the magnitude of the prescribed yaw rate, but not the magnitude of the pitch rate, is a function of the roll velocity (see eqs. (3) and (4)).

Figure 2(c) shows the response of the airplane to a 20° aileron deflection. For this case, the airplane is rolled from a steady 2g condition. The rolling for this case and all subsequent 2g cases is initiated with the flight path horizontal. An initial pitch rate of about 0.05 radian per second and an angle of attack of 10° is required for constant g flight. The trim stabilizer deflection is -3.5°. For the aileron-alone case, because of the low roll rate (an average roll rate of -0.9 radian/second), the aileron had to be held on about 7 seconds in order to roll the airplane through 360°. The small roll rate is a direct result of the large opposing rolling moment produced on the airplane by the relatively high value of the effective dihedral C_{l_β} at an angle of attack of 10°. (See table I.) Because of the low rate developed, this case does not exhibit any serious roll coupling tendencies. When i_t and δ_r are applied, a large increase in the roll velocity is noticed and, in fact, since the same aileron input was used, the airplane for this case rolled through almost $1,080^{\circ}$ of roll angle. Notice that the stabilizer and rudder deflections for this case are approximately twice as large as those shown in figure 2(a). This results from the fact that the angle of attack from which the roll is initiated in this case is exactly double that for the 1 g case. The maximum pitching and yawing velocities for $\Delta\alpha = \beta = 0$ for this case are also increased for the same reason.

Figure 2(d) shows the response of the airplane to a 30° aileron deflection, where the airplane is initially at 2g. The aileron-alone case exhibits very severe roll-coupled motions. Relatively large stabilizer and rudder deflections are needed to keep $\Delta\alpha$ and β zero because of the combination of the large angle of attack and the high roll rate developed. A sizeable increase in roll rate is noticed for the $\Delta\alpha = \beta = 0$ case.

It should be noted that in figure 2 and the subsequent figures the magnitude of the rudder and stabilizer deflections required for $\Delta\alpha = \beta = 0$ are inversely proportional to the effectiveness of the control surfaces. That is, if the control effectiveness - especially in the case of the rudder - could be increased, the corresponding deflection would be decreased. As has been pointed out in reference 5 the assumed value of $C_{n_{\delta_r}}$ (rudder effectiveness) for this airplane is only about one-third of that provided on many airplanes. However a decrease in deflection due to increased control effectiveness would not mean a reduction in the tail loads.

Effect of Ramp-Type Rudder and Stabilizer Inputs on the Airplane Response in Aileron Rolls

Using the time histories of the stabilizer and rudder deflections shown in figure 2 as a basis of the controls required for rolling with small changes in the angles of attack and sideslip, the effect of some ramp-type i_t and δ_r inputs on the rolling airplane is presented in figures 3 and 4. All the ramp rudder and stabilizer inputs were applied simultaneously with the aileron. Also, they were reversed to return them to their initial value at approximately the same time as the aileron reversal was effected. The rate for all the stabilizer deflections was assumed to be 5° per second and the rate for the rudder deflections was set at 20° per second.

Figure 3 presents a comparison of the effect of the ramp inputs with that of the exact rudder and stabilizer inputs. Figures 3(a) and 3(b) present the airplane time histories for $\left(n_g\right)_o = 1$ and $\delta_a = 20^{\circ}$ and 30°, respectively. Figure 3(c) shows the time histories for $\left(n_g\right)_o = 2$ and $\delta_a = 30^{\circ}$. The aileron-alone cases and the exact control input cases are repeated from figure 2. The magnitude of the ramp rudder and stabilizer deflections that were used in figure 3 are a rough approximation of the average values of the exact i_t and δ_r. Also, the ramps were applied in only one direction, that is, it can be seen that in the case of the rudder deflection no attempt was made to follow the exact rudder to its negative value and then back to zero. In spite of these differences from the ideal rudder and stabilizer inputs, the angles of attack and sideslip variations were considerably reduced from those obtained for the aileron-alone cases. The tendency for the α response to vary rather abruptly at the initial part of the maneuver for the ramp input cases is due mainly to the stabilizer deflection that was used. That is, because of the rate and time of application assumed for the stabilizer, this control causes the airplane initially to pitch

negatively, which results in a corresponding decrease in the angle of attack. With reference to the exact stabilizer motion, it appears that if the stabilizer deflection would have been applied at a slower rate or with some delay, smaller α changes would have been experienced. Even though the angle of attack still varied abruptly (particularly in figures 3(b) and 3(c)) when the ramp deflections were applied, the total angle of attack never reached the negative values as did the aileron-alone cases.

Since the rudder and stabilizer deflections shown in figure 3 were applied at the beginning of the roll maneuver, these results are more indicative of the effect of preventive, rather than corrective, controls. Preventive controls, as used here, are defined as controls applied in such a manner so as to prevent subsequent deviations, such as those applied with the aileron at the initiation of the roll maneuver in figure 3. Corrective controls would be applied after some deviation occurs - for instance, at $t = 1.5$ seconds for the solid curves of figure 3(a). Normally in a rolling maneuver the pilot will attempt some sort of coordination of the controls, such as the application of the rudder with the aileron to maintain small angles of sideslip. In some cases the effectiveness of rudder for controlling the sideslip may be considerably reduced due to adverse moment produced by the inertia coupling term $(I_X - I_Y)pq$. This term becomes significantly large in many cases because of the high roll rate and also the relatively large pitching velocity that is developed during rapid rolls. For example, notice the values of pitching velocity that are encountered during the aileron-alone cases shown in figure 3. High rates of pitching have also been experienced in actual flight maneuvers such as reported in references 7, 8, and 9. In fact, it is this pitching velocity coupled with the rolling velocity that produces a yawing moment opposite to that produced by the stabilizing $N_\beta \beta$. When the yawing moment due to pq becomes larger than that due to $N_\beta \beta$, rolling instability results. Proper stabilizer inputs to maintain a minimum amount of pitching during rapid rolls, which may be contrary to pilot stimuli, then should not only permit more favorable use of the rudder but should also reduce the possibility of instability due to roll coupling. This is borne out in figure 3 for the three cases shown. Also, the fact that reduction of the pitching velocity in rapid rolls tends to reduce the severity of the maneuver was pointed out in references 3 and 4, where analog results indicated that ideal pitch dampers were very effective in reducing the angles of attack and sideslip encountered in aileron rolls.

Figure 4 shows the effect of several combinations of ramp rudder and stabilizer deflections applied with the aileron. Figures 4(a), 4(c), and 4(e) present a comparison of the relative importance of the rudder and of the stabilizer when applied separately with the aileron. Figures 4(b), 4(d), and 4(f) give some indication of the sensitivity of the

rolling airplane to the magnitude of the applied stabilizer deflections. In figure 4(a) for $\left(n_g\right)_o = 1$ and $\delta_a = 20^\circ$, it can be seen that all three of the control combinations were effective in reducing the α and β motions during the recovery phase of the maneuver. With the exception of the first negative variation of $\Delta\alpha$, the angles of attack and sideslip variations for $\delta_r = 0$ are nearly the same as those obtained when both the rudder and stabilizer are applied with the aileron. It should be noted that even though the $\Delta i_t = 0$ case exhibits small angles of attack and sideslip variations these results should be evaluated in light of the low level of roll rate experienced for this case. That is, since the low roll rate is responsible, in part, for the small variations it is probable that if a larger aileron deflection were used in this case to produce a larger roll rate the angles of attack and sideslip variations would also be increased. It appears that if a comparatively high rate of rolling is required the stabilizer applied with the aileron is at least as effective, and in some cases (see figs. 4(c) and 4(e)) more effective, in maintaining small variations in the angles of attack and sideslip than the rudder applied with the aileron.

Since the stabilizer when applied in combination with the rudder and aileron appears to be quite effective in reducing the angles of attack and sideslip variations, it is important to know how sensitive the airplane at this flight condition is to the magnitude of the stabilizer deflection. Figure 4(b) shows three values of Δi_t with $\delta_r = 10^\circ$ for $\left(n_g\right)_o = 1$ and $\delta_a = 20^\circ$. Even though the angles of attack and sideslip variations are directly dependent on the magnitude of Δi_t, all three cases offer a definite improvement, especially during the recovery phase, over the aileron-alone case shown in figure 3(a). Although the range of values shown here for Δi_t is small, it should be remembered that the Δi_t per g is about 1.7°. Thus a pilot, because of this high sensitivity of the control, could probably distinguish between say 1° or 3° of stabilizer deflection. It is also interesting to note the effect that the longitudinal control (Δi_t) has on the lateral variables, namely, yawing velocity and sideslip angle. The difference in the yaw rate and, consequently, the sideslip is attributed to the $(I_X - I_Y)pq$ term in the yawing-moment equation. The angle-of-attack response during the initial part of the maneuver is seen to be proportional to the magnitude of Δi_t. This effect was mentioned in the discussion of figure 3.

Figure 4(c) shows the effect of the rudder and stabilizer deflections for an aileron input of 30° and $\left(n_g\right)_o = 1$. Note that for $\Delta i_t = 0$ the rudder input of 15° is not sufficient to yaw the airplane favorably

during the complete maneuver. However, when both the stabilizer and rudder are applied the pitch rate is reduced, thereby reducing the yawing moment due to pq and the resulting yawing is mostly negative. Again, the angles of attack and sideslip variations for $\delta_r = 0$ are only slightly different from those obtained when both the rudder and stabilizer are applied. Figure 4(d) presents results similar to those of figure 4(b) for $\left(n_g\right)_o = 1$ and $\delta_a = 30^\circ$. Note again the proportional change in the yawing rate with the magnitude of Δi_t.

Figures 4(e) and 4(f) show the airplane response to $\delta_a = 30^\circ$ and combinations of rudder and stabilizer deflections for $\left(n_g\right)_o = 2$. The results shown in figure 4(e) indicate that the stabilizer when applied with the aileron maintained smaller values of β than for the case of the rudder and aileron combination, even though the level of roll rate for the $\delta_r = 0$ is much higher than that for $\Delta i_t = 0$. Figure 4(f) presents the effect of two different stabilizer deflections applied with both δ_r and δ_a equal to 30° and $\left(n_g\right)_o = 2$. The angles of attack and sideslip variations for both the Δi_t's show a large reduction from the aileron case of figure 3(c).

Effects of Automatic Controls Designed To Minimize the Angles of Attack and Sideslip Variations in Rapid Rolls

The human pilot, even though he has some idea of the rudder and stabilizer deflections necessary to maintain small variations in the angles of attack and sideslip during aileron rolls, may still be unable to cope with the complexity and rapidity of the motions that are encountered in such maneuvers. Therefore, it may become necessary to resort to some type of automatic control. A brief investigation has been made which considers the rudder and stabilizer as defined by equations (13) and (14), respectively, as possible automatic controls. In this investigation, the automatic control inputs were assumed to be perfect in that zero time lag was assumed for the control servos. Also, no limitations of rate or magnitude were assumed for either the rudder or stabilizer motion.

In the analysis, for the sake of simplification, the expressions defining the automatic rudder and stabilizer were derived from the airplane equations of motion for principal body axes. In practice, as was mentioned previously, the instruments for sensing the values of p, $\dot{p}$, and α_o, which are required for the automatic rudder and stabilizer,

would be alined to record these quantities about the principal axis. In the analog investigation of the automatic controls, the airplane configuration that was used was assumed to have the same characteristics as those presented in table I with the exception of I_{XZ}, which was taken as zero.

The effects of the rudder and stabilizer inputs as defined by equations (13) and (14) are presented in figure 5. Figure 5(a) shows the effect on the airplane response for $\delta_a = 20^\circ$ when the airplane is initially at 1 g. It can be seen that angles of attack and sideslip variations remain almost zero when the stabilizer and rudder are operating. Since these results are very similar to those presented in figure 2(a) for the exact controls, the assumptions used in simplifying the exact control expressions to obtain equations (13) and (14) are apparently valid for this airplane and flight condition. The maximum incremental stabilizer deflection required is approximately 2° and the rudder reaches maximum values of 14° and -9°. The roll rate response is somewhat improved when the stabilizer and rudder are operating. This improvement, as was indicated in a previous section, is mainly the result of almost zero dihedral effect due to the practically zero β during the maneuver. Figure 5(b) presents the control inputs for $\left(n_g\right)_o = 1$ and $\delta_a = 30^\circ$. The magnitude of the stabilizer and rudder deflections is increased from the $\delta_a = 20^\circ$ case because of the higher roll rate developed for the larger aileron deflection. Figure 5(c) shows the airplane time histories when the airplane is rolled from 2g trim flight. For the $\delta_a = 30^\circ$ aileron-alone case the airplane rolled only about 200° and therefore experienced a somewhat less violent maneuver than the 360° rolls previously presented for this flight condition. Two aileron deflections were considered with the automatic controls operating. For $\delta_a = 30^\circ$, it can be seen that the roll rate is markedly increased when the rudder and stabilizer are operating. Because of this high rate of rolling and the relatively large angle of attack from which the roll is initiated, the necessary rudder and stabilizer deflections are large. Such control deflections may be unattainable or impractical because of the excessive loads they might produce on the tail surfaces. Some calculations of the loads are discussed briefly in the next section. Since a significant increase is generally obtained in the roll rate for a particular aileron deflection when the automatic controls are used, a smaller aileron deflection may be sufficient to produce the roll rate required for a specific maneuver. For $\delta_a = 20^\circ$ and the automatic controls operating the roll rate developed is still higher than that shown for $\delta_a = 30^\circ$ with aileron alone. The necessary stabilizer and rudder deflections for this case ($\delta_a = 20^\circ$) are considerably less than those required for $\delta_a = 30^\circ$.

Effect of the Automatic Controls on Tail Loads

Rolling an airplane with small variations in the angles of attack and sideslip by proper rudder and stabilizer inputs does not guarantee that loads on the tail surfaces will necessarily be small. The rudder and stabilizer deflections required for maintaining the small variations may produce loads which are larger than those experienced for zero control deflections and varying angles of attack and sideslip. In order to determine the loads produced on the tail surfaces when the automatic rudder and stabilizer are utilized, the maximum loads on the vertical and horizontal tails were calculated for the aileron rolls presented in figure 5.

Listed in table II(a) are the maximum positive and negative tail loads computed for the two g conditions and two aileron deflections. Presented in table II(b) are the assumed tail characteristics and expressions that were used for calculating the horizontal and vertical tail loads. It should be pointed out that the loads listed for the cases where the automatic controls are not operating are mainly due to the attitude and angular motions of the airplane, whereas the loads listed for the cases of the controls operating are principally due to the magnitude of the rudder or stabilizer deflections. An initial load is given for the horizontal tail in each case, which is produced by the initial or trim values of α and i_t. No negative loads are indicated for the horizontal tail when the automatic controls are operating since the loads experienced for these inputs always remain positive. For both aileron deflections at $\left(n_g\right)_o = 1$, the maximum loads are reduced when the automatic controls are operating. However, at $\left(n_g\right)_o = 2$ and $\delta_a = 30^\circ$ (fig. 5(c)), only the vertical tail loads show a reduction with the automatic rudder and stabilizer. The increase in the horizontal tail load is due mainly to the comparatively large stabilizer deflection required. However, since the magnitude of the controls is proportional to the magnitude of the roll rate developed, if an aileron deflection of 20° is applied for this condition the control deflections are considerably reduced, even though the roll rate is greater than that for the case of $\delta_a = 30^\circ$ without automatic control. The last row in table II(a) lists the loads experienced for $\delta_a = 20^\circ$ and $\left(n_g\right)_o = 2$ with the automatic rudder and stabilizer operating. Comparing these loads with those for $\delta_a = 30^\circ$ and $\left(n_g\right)_o = 2$ without the automatic controls shows a substantial reduction in both the horizontal and vertical tail loads when the automatic rudder and stabilizer are applied.

CONCLUDING REMARKS

Expressions have been derived from the five-degree-of-freedom airplane equations of motion which define the rudder and stabilizer motions necessary to maintain constant angle of attack and zero sideslip during an aileron roll. The control motions calculated by using these expressions are useful in determining the magnitude and direction of the rudder and stabilizer deflections that might be applied by a pilot or by automatic controls to maintain small variations in aileron rolls.

For the airplane configuration and flight condition investigated, simple ramp-type rudder and stabilizer deflections, applied with the aileron and similar to the exact inputs in magnitude and direction, were effective in reducing the angles of attack and sideslip in rapid rolls. The ramp stabilizer deflections applied with the aileron were nearly as effective as the rudder and stabilizer deflections for the cases investigated.

The expressions defining the exact rudder and stabilizer necessary for zero variation of the angles of attack and sideslip during rolling were simplified and considered as the basis for automatic controls. For the airplane configuration and flight condition investigated, and assuming no rate or magnitude limitations and zero time lag for the control inputs, the automatic rudder and stabilizer controls were very effective in reducing the angles of attack and sideslip developed during rolling. The roll rate was increased and the roll rate response was considerably improved when the automatic controls were applied. The automatic controls generally reduced the maximum loads experienced by the vertical and horizontal tail surfaces during the aileron rolls.

Langley Aeronautical Laboratory,
National Advisory Committee for Aeronautics,
Langley Field, Va., January 10, 1957.

REFERENCES

1. Phillips, William H.: Effect of Steady Rolling on Longitudinal and Directional Stability. NACA TN 1627, 1948.

2. White, R. J., Uddenberg, R. C., Murray, D., and Graham, F. D.: The Dynamic Stability and Control Equations of a Pivoted-Wing Supersonic Pilotless Aircraft, With Downwash, Wake and Interference Effects Included. Doc. No. D-8510, Boeing Aircraft Co., Jan. 9, 1948.

3. Weil, Joseph, and Day, Richard E.: An Analog Study of the Relative Importance of Various Factors Affecting Roll Coupling. NACA RM H56A06, 1956.

4. Gates, Ordway B., Jr., Weil, Joseph, and Woodling, C. H.: Effect of Automatic Stabilization on the Sideslip and Angle-of-Attack Disturbances in Rolling Maneuvers. NACA RM L55E25b, 1955.

5. Phillips, William H.: Analysis of an Automatic Control To Prevent Rolling Divergence. NACA RM L56A04, 1956.

6. Gates, Ordway B., Jr., and Woodling, C. H.: A Theoretical Analysis of the Effects of Engine Angular Momentum on Longitudinal and Directional Stability in Steady Rolling Maneuvers. NACA RM L55G05, 1955.

7. Finch, Thomas W., Peele, James R., and Day, Richard E.: Flight Investigation of the Effect of Vertical-Tail Size on the Rolling Behavior of a Swept-Wing Airplane Having Lateral-Longitudinal Coupling. NACA RM H55L28a, 1956.

8. Sisk, Thomas R., and Andrews, William H.: Flight Experience With a Delta-Wing Airplane Having Violent Lateral-Longitudinal Coupling in Aileron Rolls. NACA RM H55H03, 1955.

9. Stone, Ralph W., Jr.: Some Notes on the Violent Lateral-Longitudinal Coupling Motions of the Douglas X-3 Airplane in Aileron Rolls. NACA RM L56C15, 1956.

TABLE I

STABILITY DERIVATIVES, MASS CHARACTERISTICS OF THE AIRPLANE,

AND OTHER CONSTANTS USED IN THE STUDY

I_X, slug-ft^2	10,976
I_Y, slug-ft^2	57,100
I_Z, slug-ft^2	64,975
I_{XZ}, slug-ft^2	942
q, lb/ft^2	197
S, ft^2	376
b, ft	36.6
$\bar{c}$, ft	11.32
W, lb	23,900
m, slugs	742
V, ft/sec	691
h, ft	32,000
ρ, slug/ft^3	0.000826
Mach number	0.7
ϵ, deg	1
$I_{X_e}\omega_e$, slug-ft^2/sec	17,554
$C_{l_{\delta_a}}$, per radian	-0.0528
C_{l_p}, per radian	-0.255
C_{l_r}, per radian	0.042
$C_{m_{i_t}}$, per radian	-1.0
C_{m_q}, per radian	-3.5
$C_{m_{\dot{\alpha}}}$, per radian	-1.5
C_{m_α}, per radian	-0.36
$C_{n_{\delta_a}}$, per radian	0
$C_{n_{\delta_r}}$, per radian	-0.03
C_{n_r}, per radian	-0.095
C_{n_p}, per radian	0
C_{n_β}, per radian	0.057
C_{Y_β}, per radian	-0.50
C_{L_α}, per radian	3.85

$C_{l_\beta}(\alpha)$ . . . .

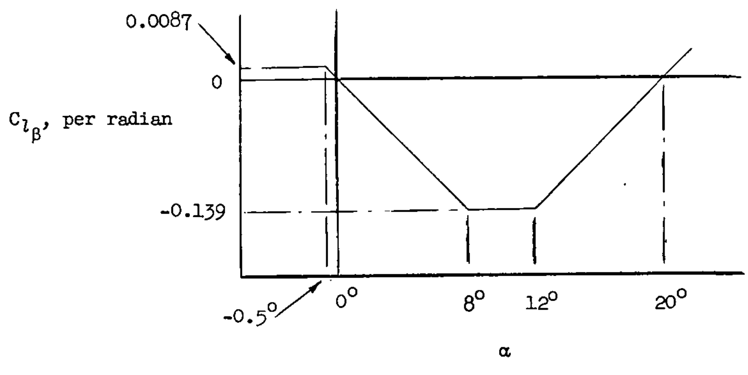

TABLE II

TAIL LOADS DURING RAPID ROLLS

(a) Comparison of the maximum tail loads experienced with and without the automatic controls

Automatic rudder and stabilizer	Horizontal tail loads, lb			Vertical tail loads, lb	
	Initial	Maximum negative	Maximum positive	Maximum positive	Maximum negative
$\left(n_g\right)_o = 1;\ \delta_a = 20^\circ$					
Not operating	990	3,792	8,148	5,555	3,437
Operating	990	-----	3,383	1,452	548
$\left(n_g\right)_o = 1;\ \delta_a = 30^\circ$					
Not operating	990	4,273	6,789	5,126	2,881
Operating	990	-----	5,313	1,985	733
$\left(n_g\right)_o = 2;\ \delta_a = 30^\circ$					
Not operating	2,002	1,594	8,931	5,926	2,859
*Operating	2,002	-----	11,336	3,718	1,741
$\left(n_g\right)_o = 2;\ \delta_a = 20^\circ$					
Operating	2,002	-----	6,599	2,726	1,526

*The large load listed for this case is primarily due to the large increase in roll rate from the not-operating case (see fig. 5(c)). When $\delta_a = 20^\circ$ was used for this g condition, which still resulted in a larger roll rate than the not-operating, $\delta_a = 30^\circ$, case, a reduction in the horizontal as well as the vertical tail loads was experienced.

TABLE II.- CONCLUDED

TAIL LOADS DURING RAPID ROLLS

(b) Horizontal and vertical tail characteristics and expressions used for calculating the tail loads

Horizontal Tail:

C_{L_α} (based on wing area), per radian	0.755
Longitudinal distance from center of gravity to $\bar{c}/4$ of horizontal tail, x_{ht}, ft	15.0
Rate of change of downwash angle with angle of attack, $d\epsilon/d\alpha$	0.43

$$\text{Load}_{ht}\ (\text{lb}) = \frac{\rho V^2 S}{2} C_{L_\alpha}\left[\alpha_{cg}\left(1 - \frac{d\epsilon}{d\alpha}\right) + \frac{x_{ht}}{V} q + i_t\right]$$

Vertical Tail:

C_{Y_β} (based on wing area), per radian	-0.23
$C_{Y_{\delta_r}}$ (based on wing area), per radian	0.074
Longitudinal distance from center of gravity to $\bar{c}/4$ of vertical tail, x_{vt}, ft	14.8
Vertical distance from fuselage reference line to $\bar{c}/4$ of vertical tail, z_{vt}, ft	5.6

$$\text{Load}_{vt}\ (\text{lb}) = \frac{\rho V^2 S}{2}\left[C_{Y_\beta}\left(\beta_{cg} - \frac{x_{vt}}{V} r + \frac{z_{vt}}{V} p\right) + C_{Y_{\delta_r}} \delta_r\right]$$

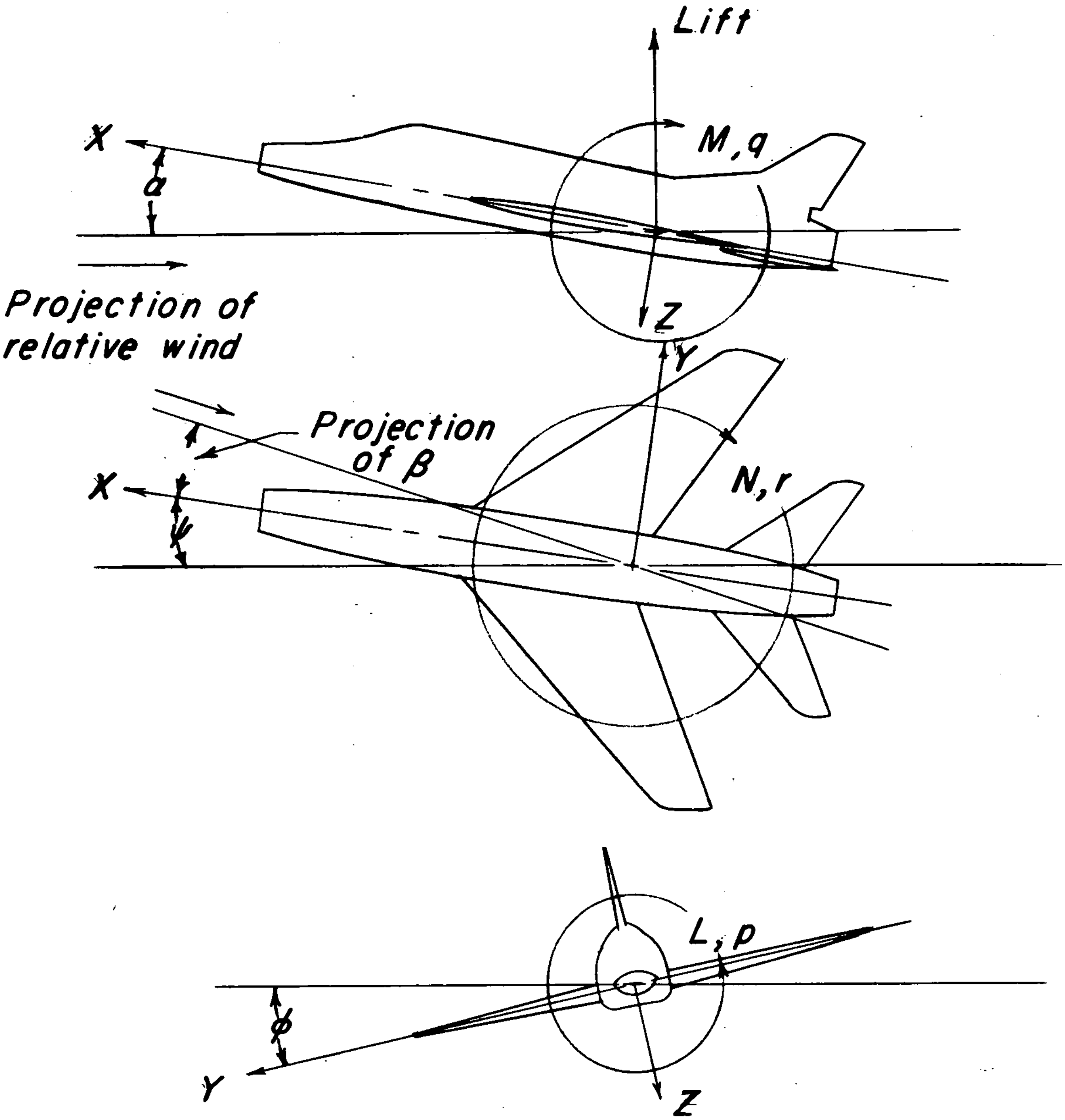

Figure 1.- Sketch showing the body axis system. Each view presents a plane of the axis system as viewed along the third axis.

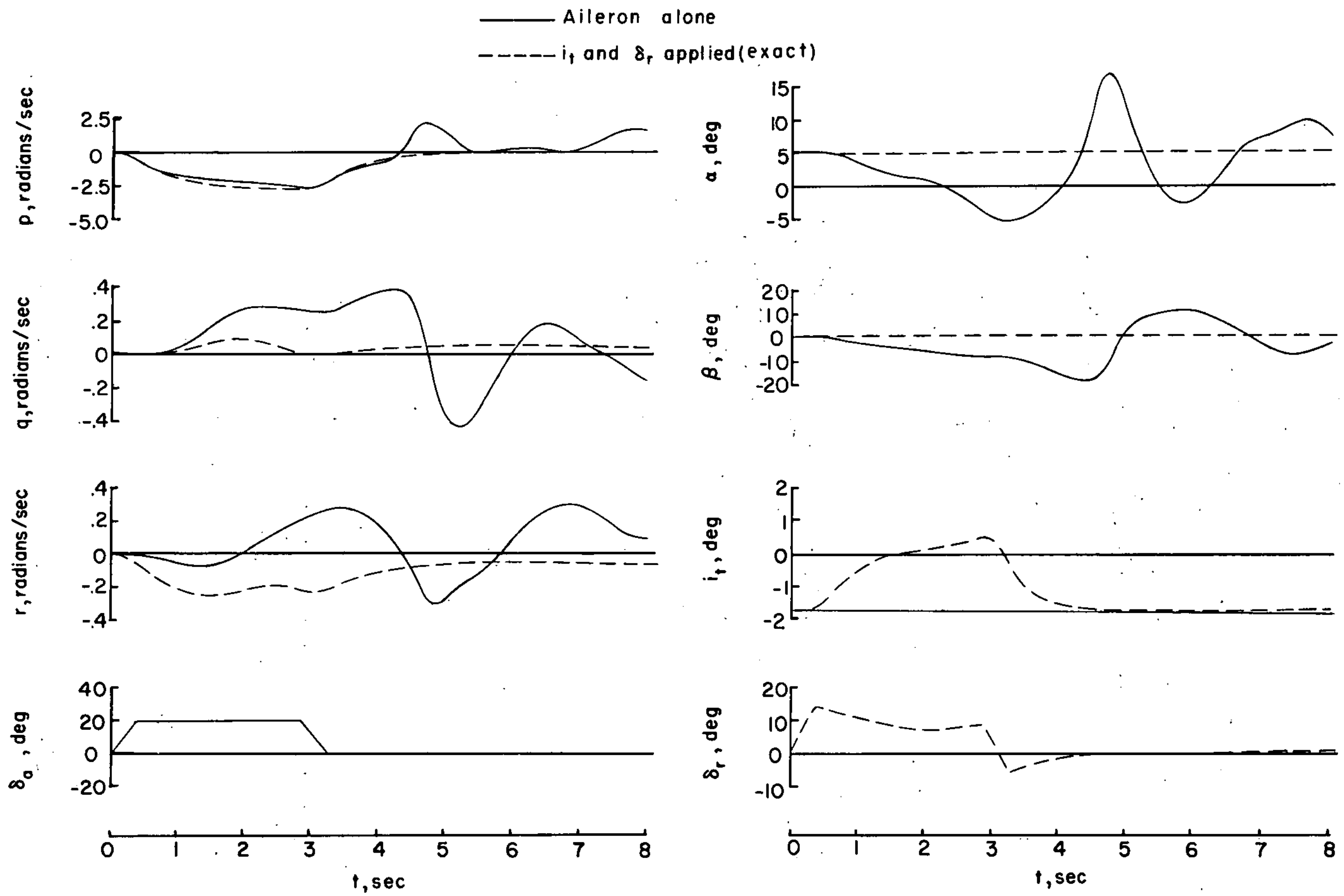

(a) $\left(n_g\right)_o = 1$; $\delta_a = 20^\circ$.

Figure 2.- Airplane response to aileron input with and without exact stabilizer and rudder required for $\Delta\alpha = \beta = 0$.

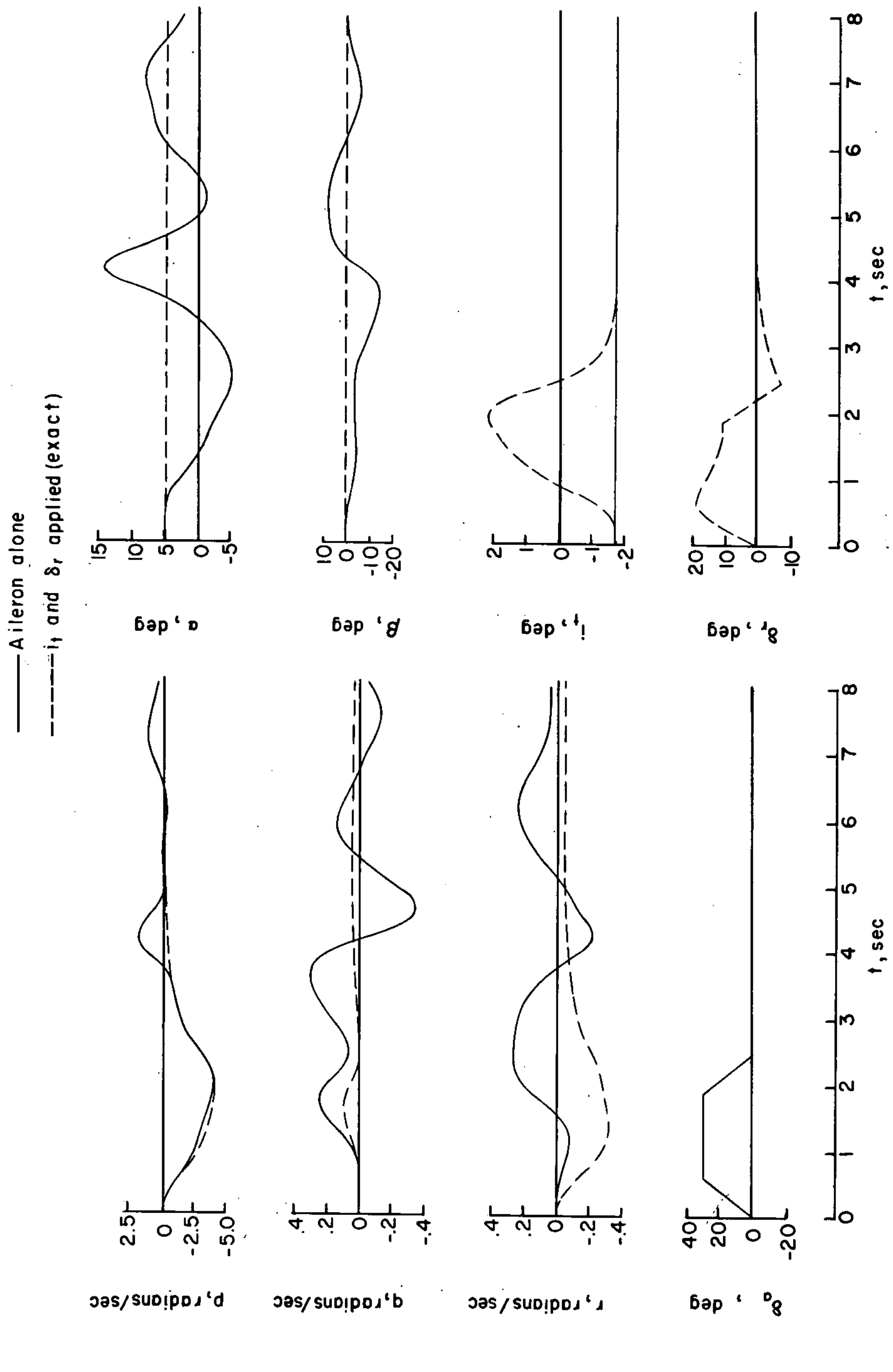

(b) $(n_g)_o = 1$; $\delta_a = 30^\circ$.

Figure 2.- Continued.

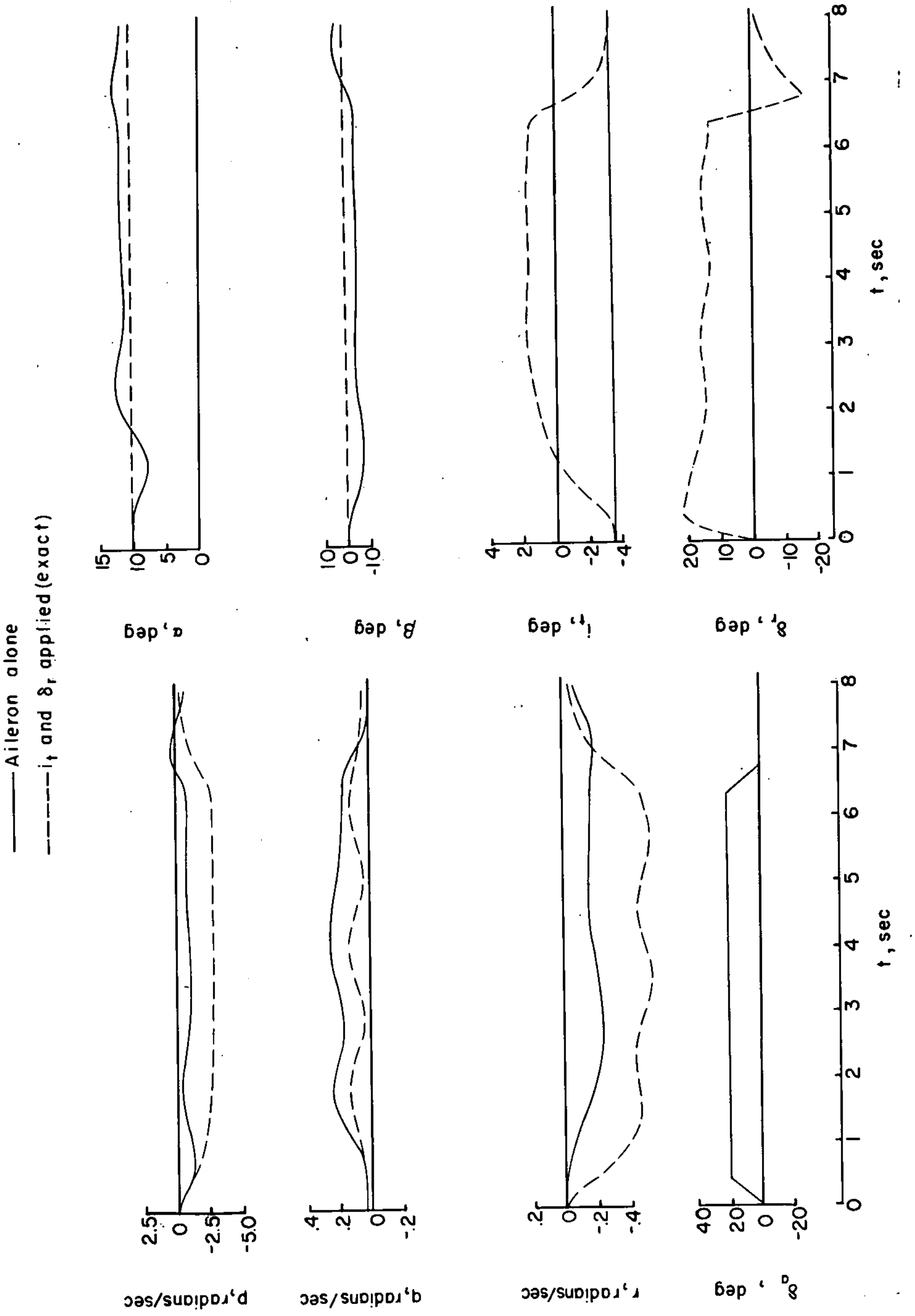

(c) $(n_g)_o = 2;\ \delta_a = 20^\circ$.

Figure 2.- Continued.

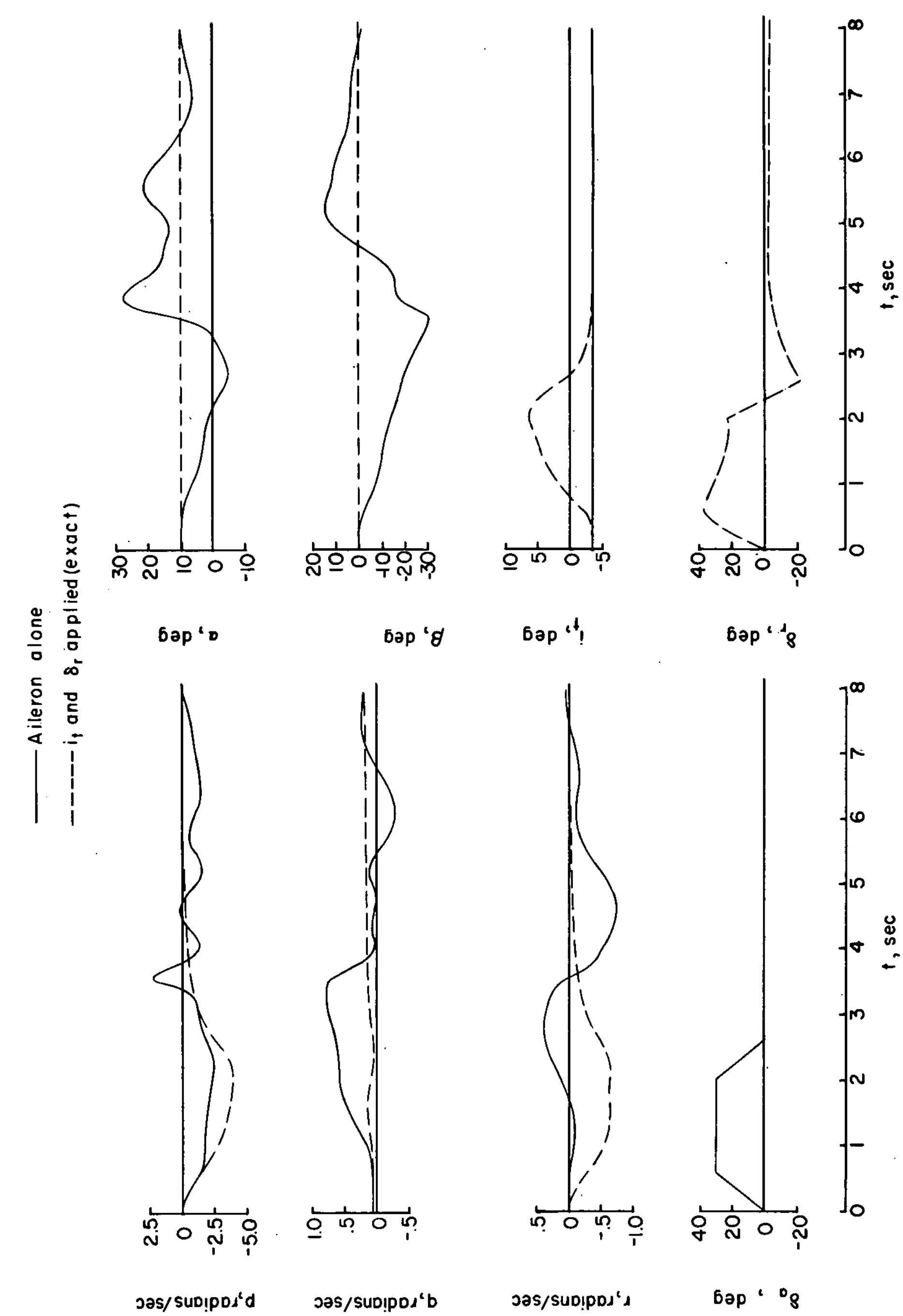

(d) $(n_g)_o = 2$; $\delta_a = 30^\circ$.

Figure 2.- Concluded.

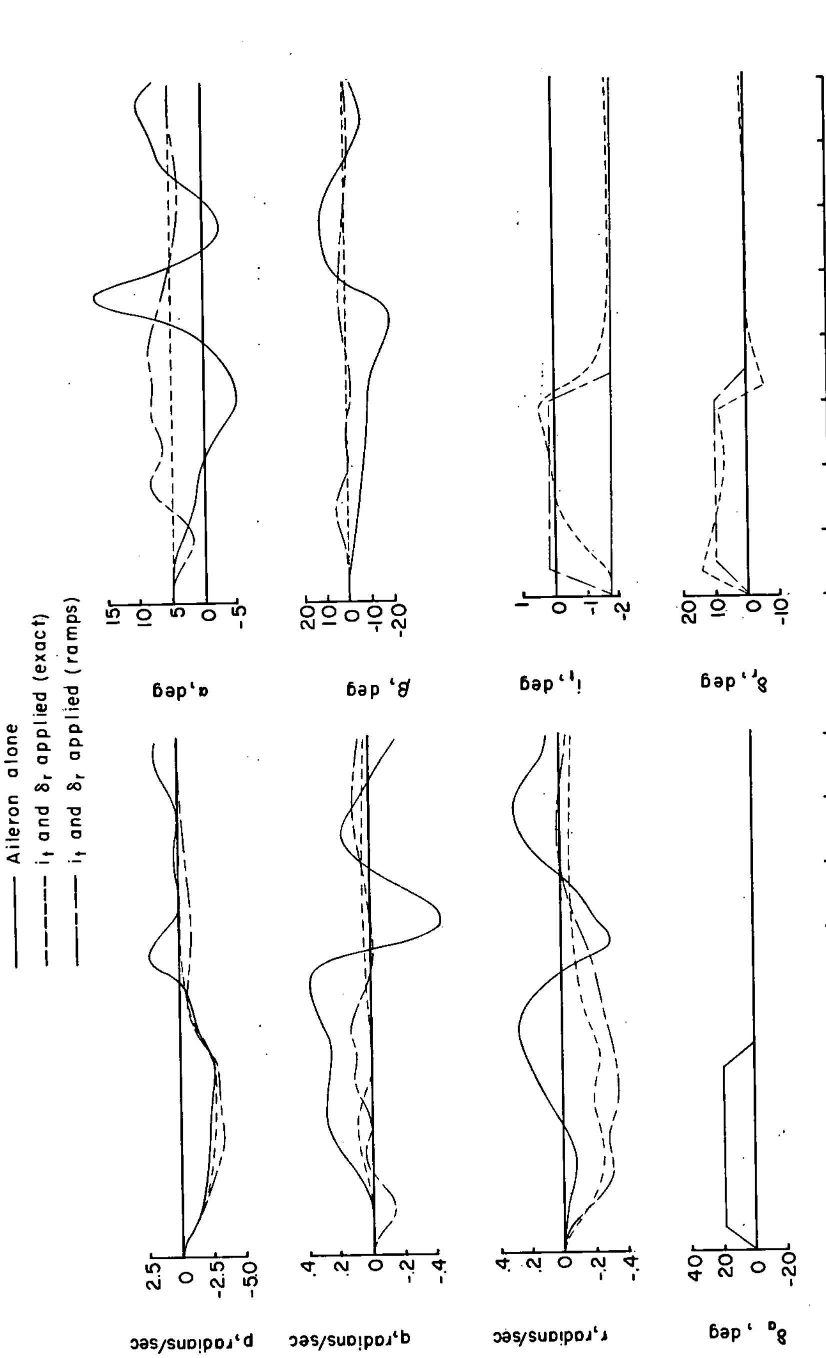

(a) $(n_g)_o = 1$; $\delta_a = 20^{\circ}$.

Figure 3.- Comparison of the exact rudder and stabilizer inputs with ramp-type rudder and stabilizer inputs and their effect on the rolling airplane.

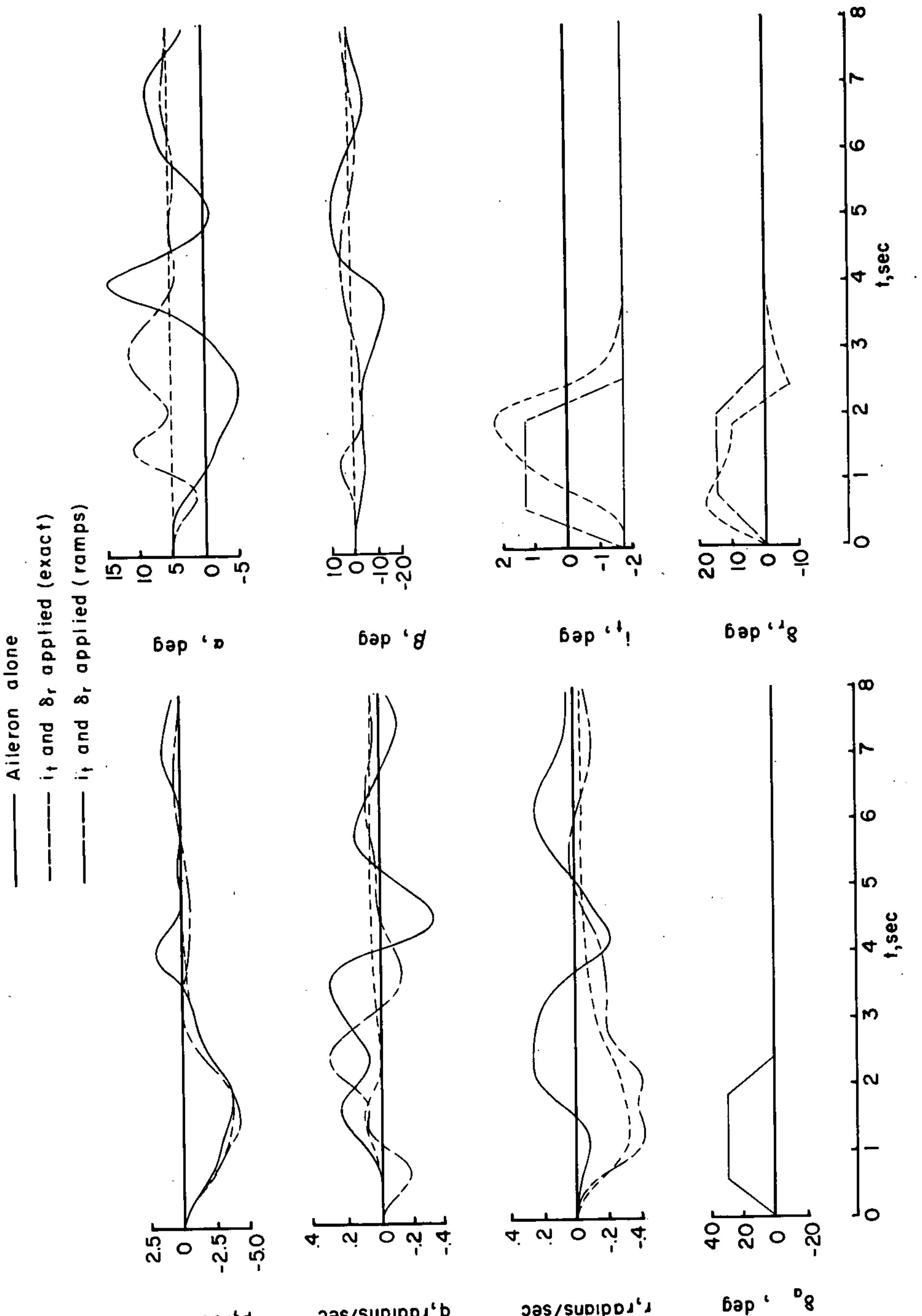

(b) $(n_g)_o = 1$; $\delta_a = 30^\circ$.

Figure 3.- Continued.

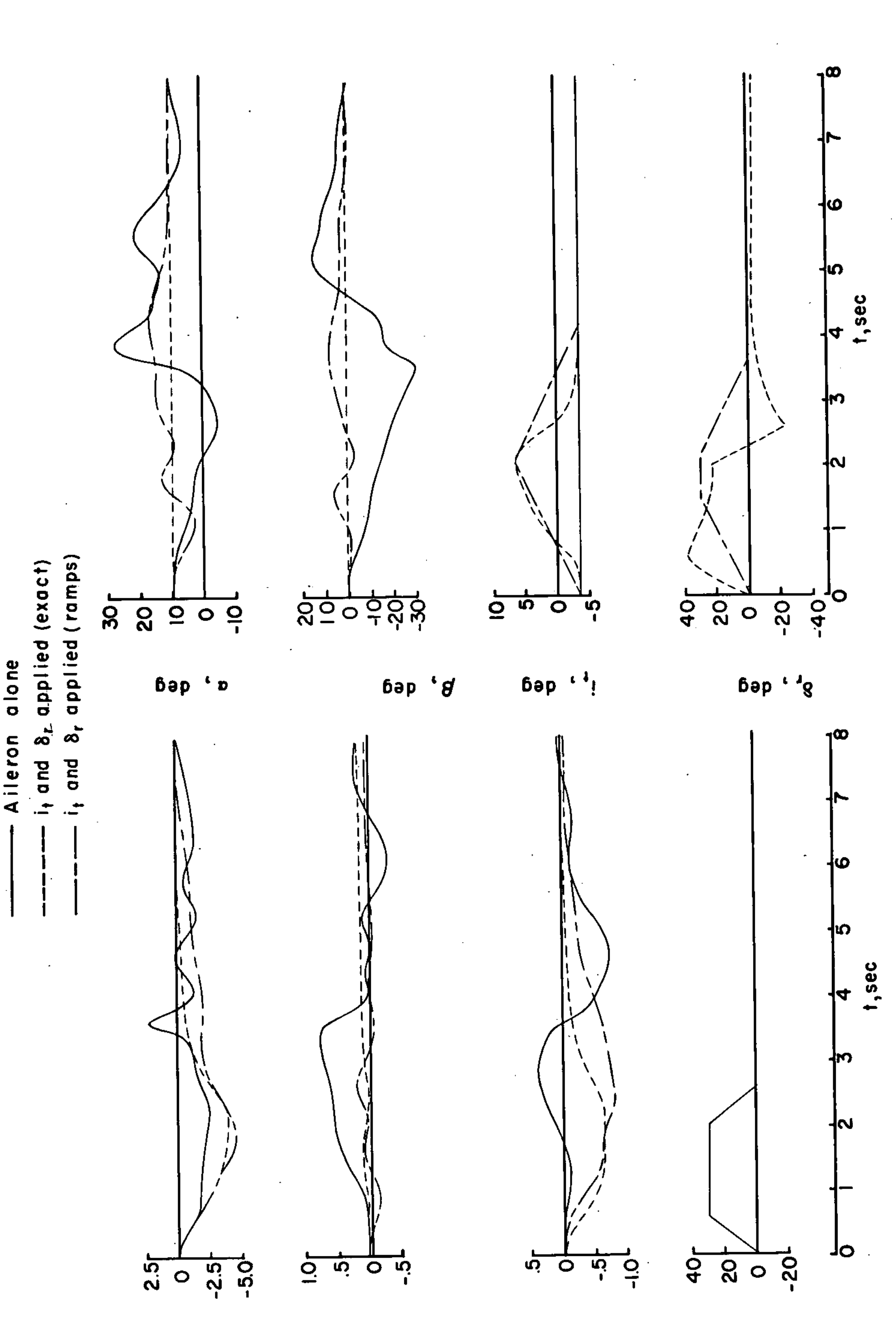

(c) $(n_g)_o = 2$; $\delta_a = 30^{\circ}$.

Figure 3.- Concluded.

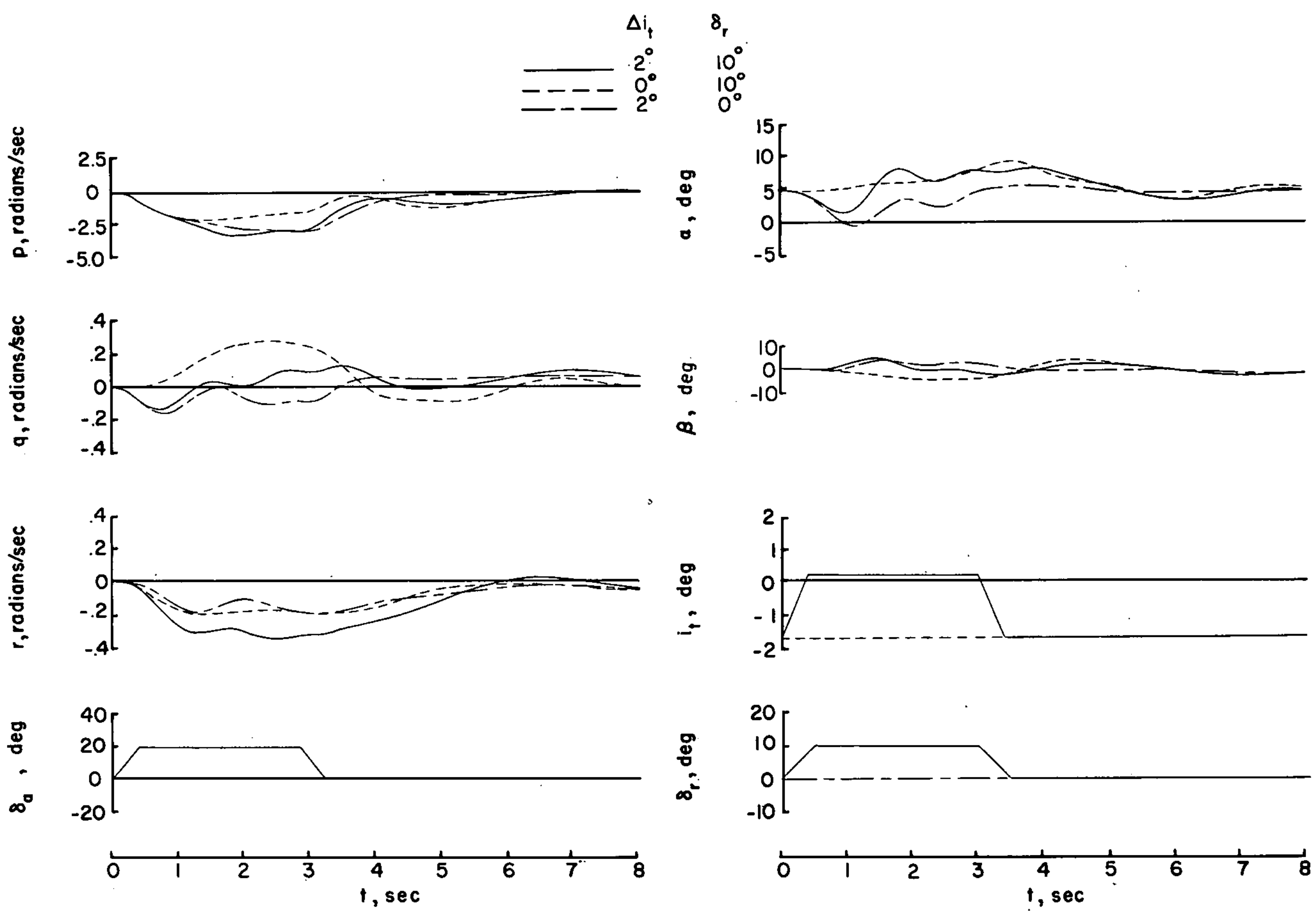

(a) $(n_g)_o = 1$; $\delta_a = 20°$.

Figure 4.- Effect of ramp-type rudder and stabilizer inputs on the airplane response in aileron rolls.

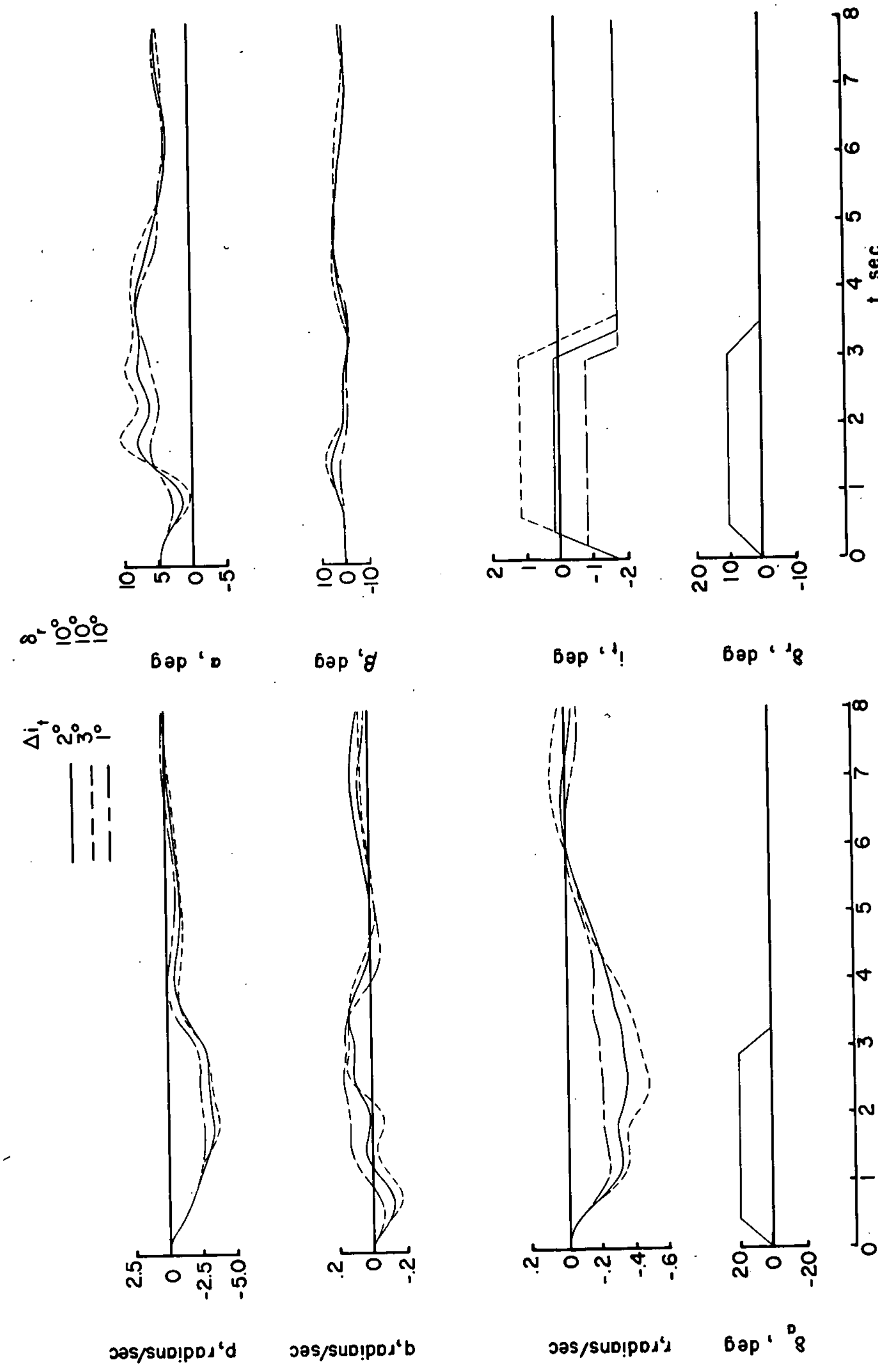

(b) $(n_g)_o = 1$; $\delta_a = 20°$.

Figure 4.- Continued.

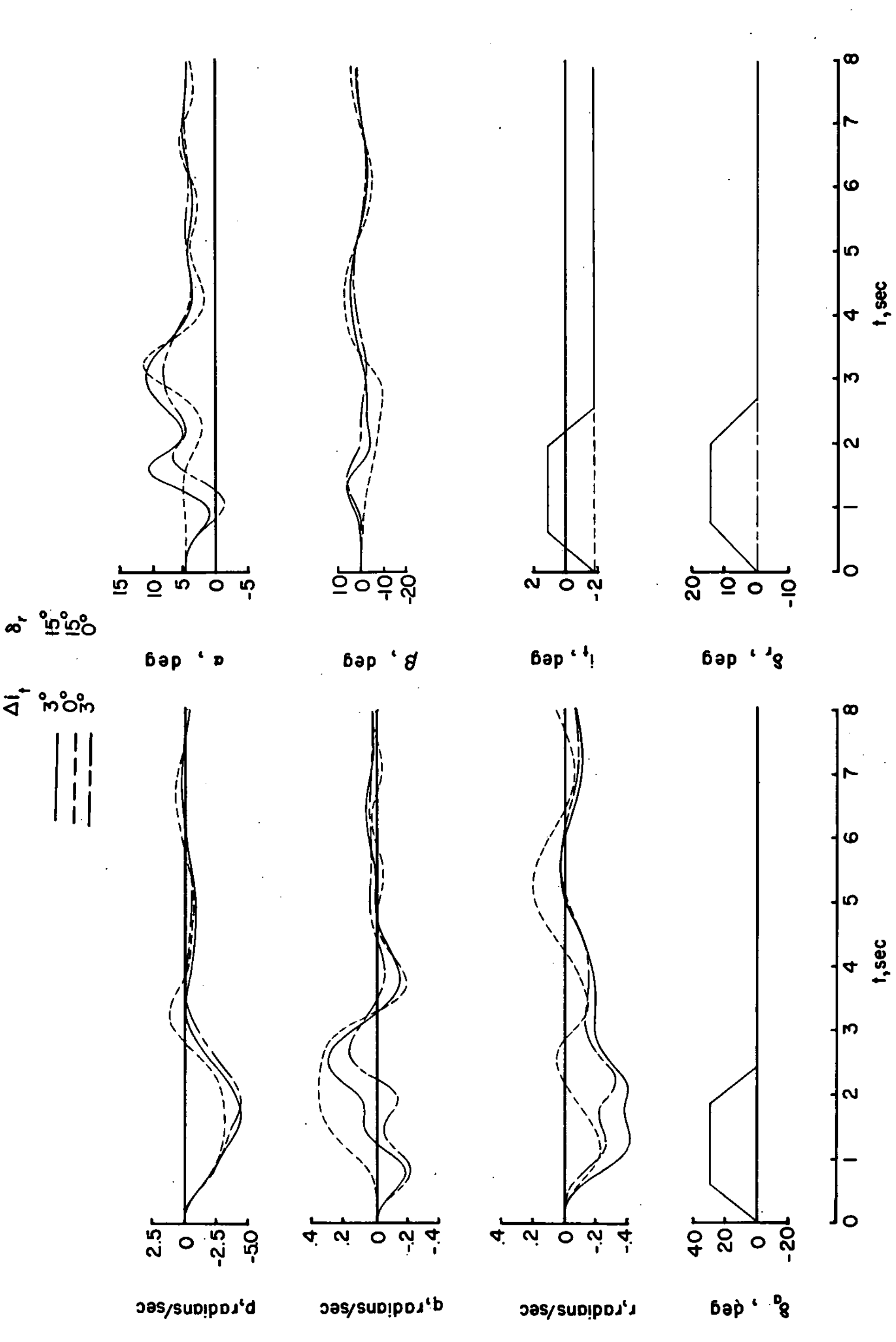

(c) $\left(n_g\right)_o = 1$; $\delta_a = 30^\circ$.

Figure 4.- Continued.

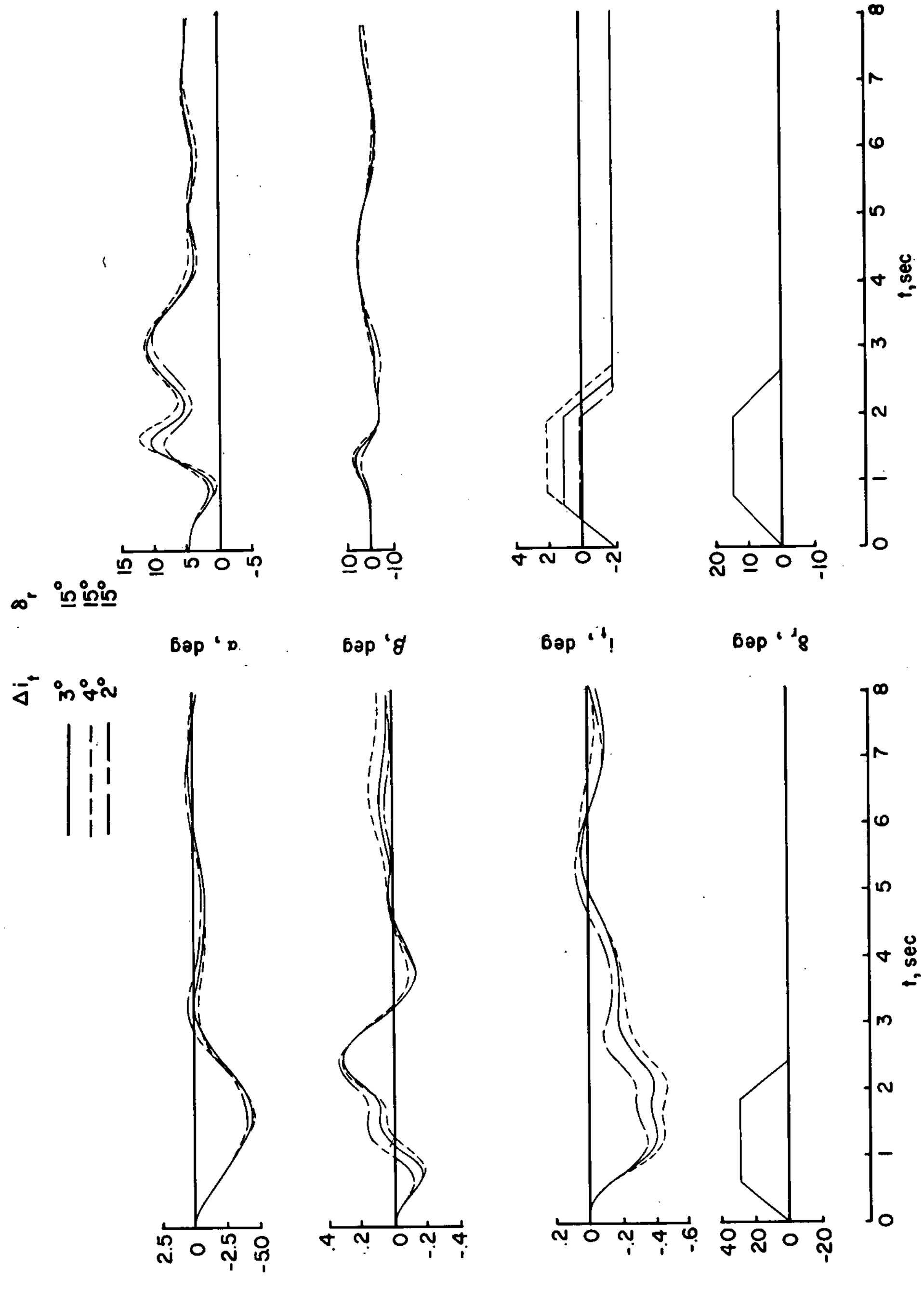

(d) $\left(n_g\right)_o = 1$; $\delta_a = 30^{\circ}$.

Figure 4.- Continued.

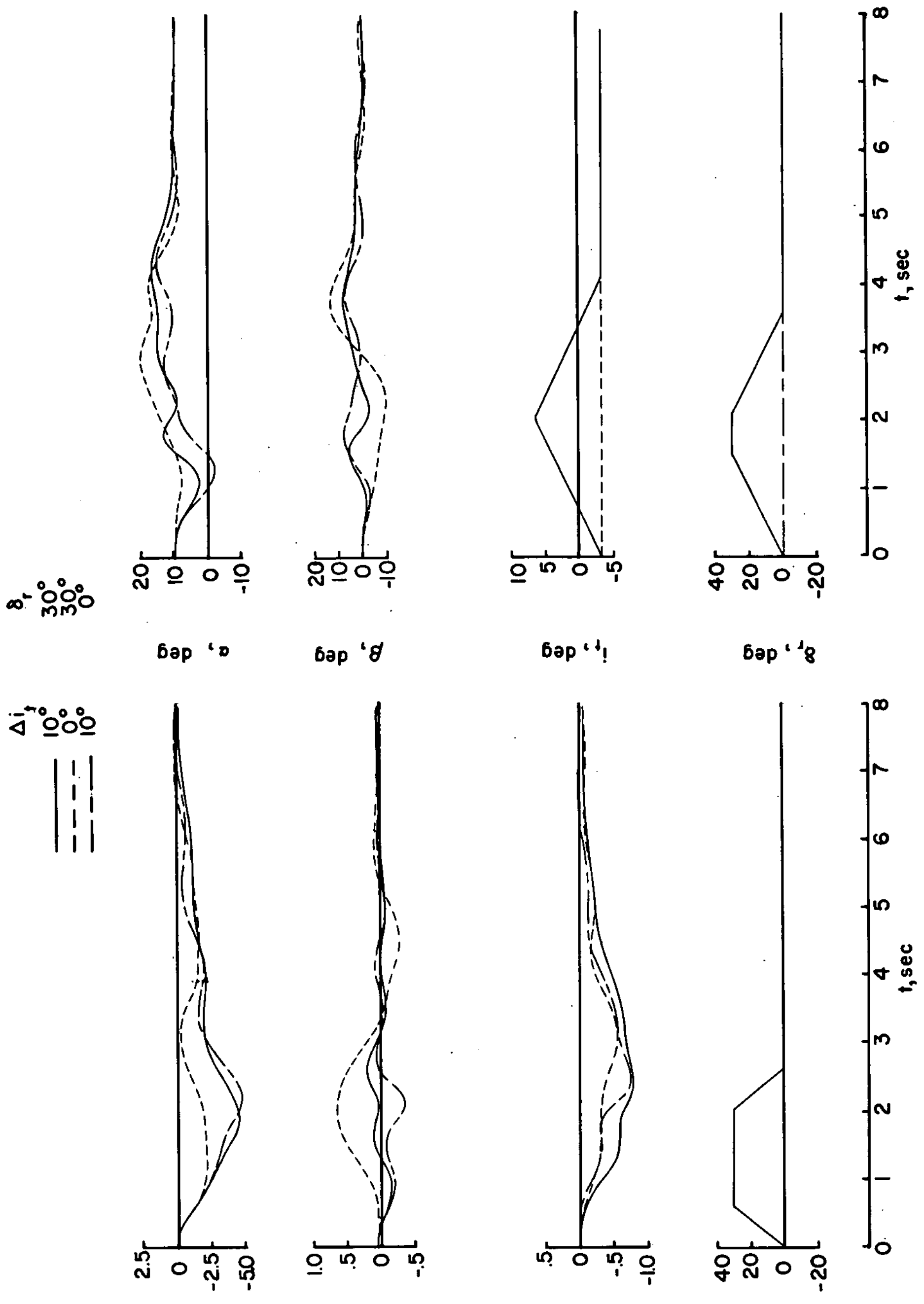

(e) $(n_g)_o = 2;\ \delta_a = 30^{\circ}$.

Figure 4.- Continued.

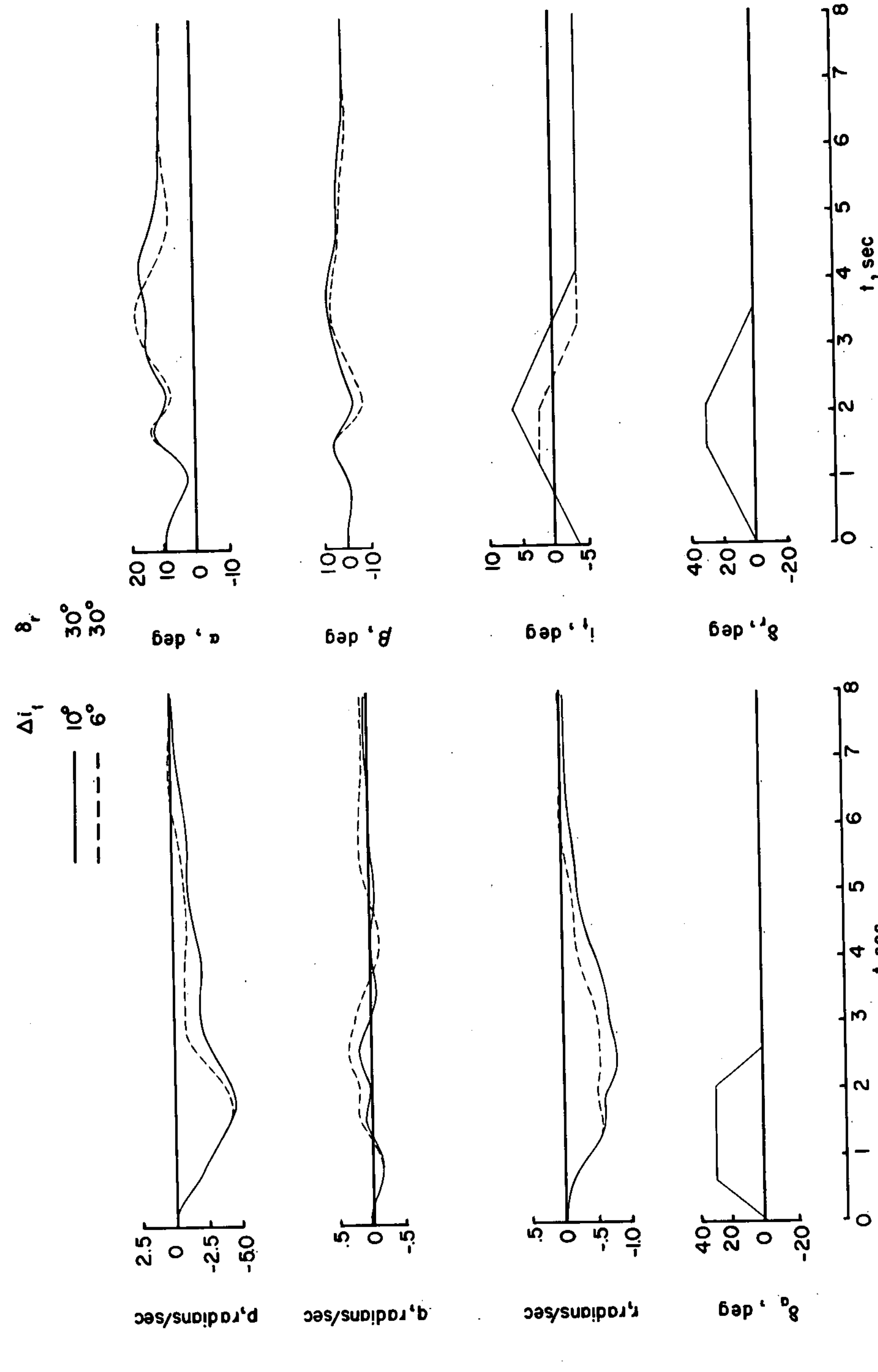

(f) $(n_g)_o = 2$; $\delta_a = 30^{\circ}$.

Figure 4.- Concluded.

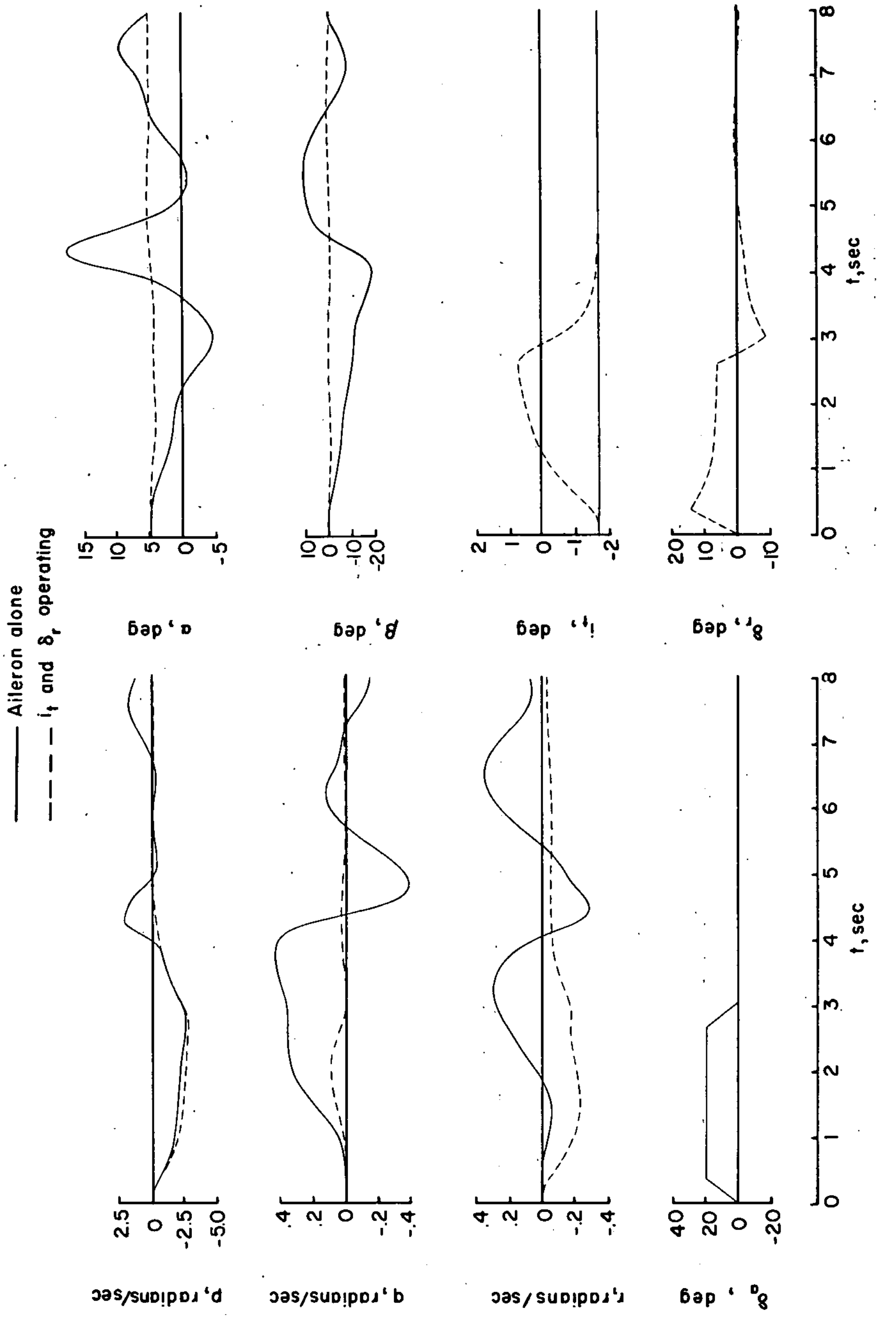

(a) $(n_g)_o = 1$; $\delta_a = 20^\circ$.

Figure 5.- Effect of automatic rudder and stabilizer on the airplane response in aileron rolls.

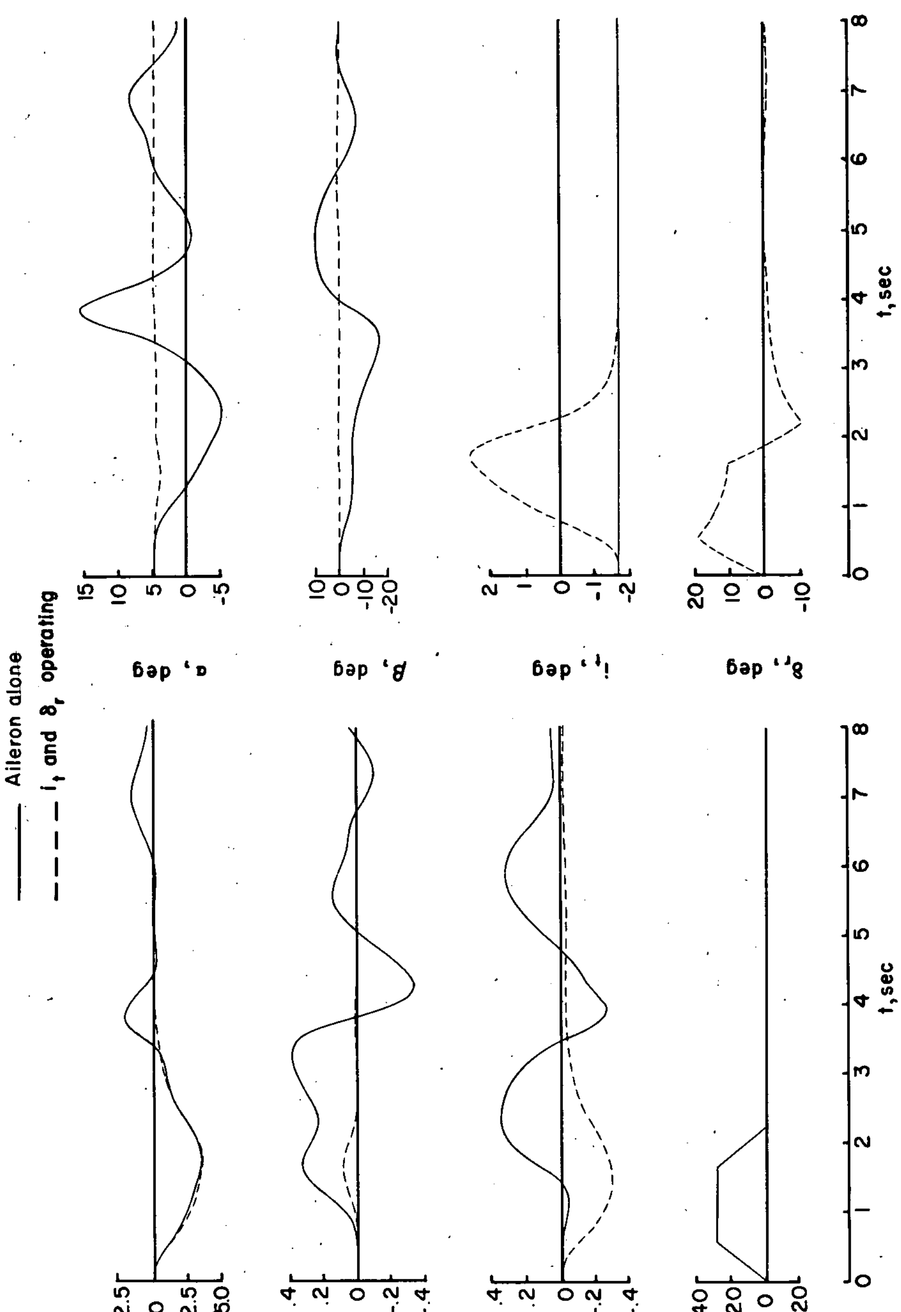

(b) $(n_g)_o = 1$; $\delta_a = 30^\circ$.

Figure 5.- Continued.

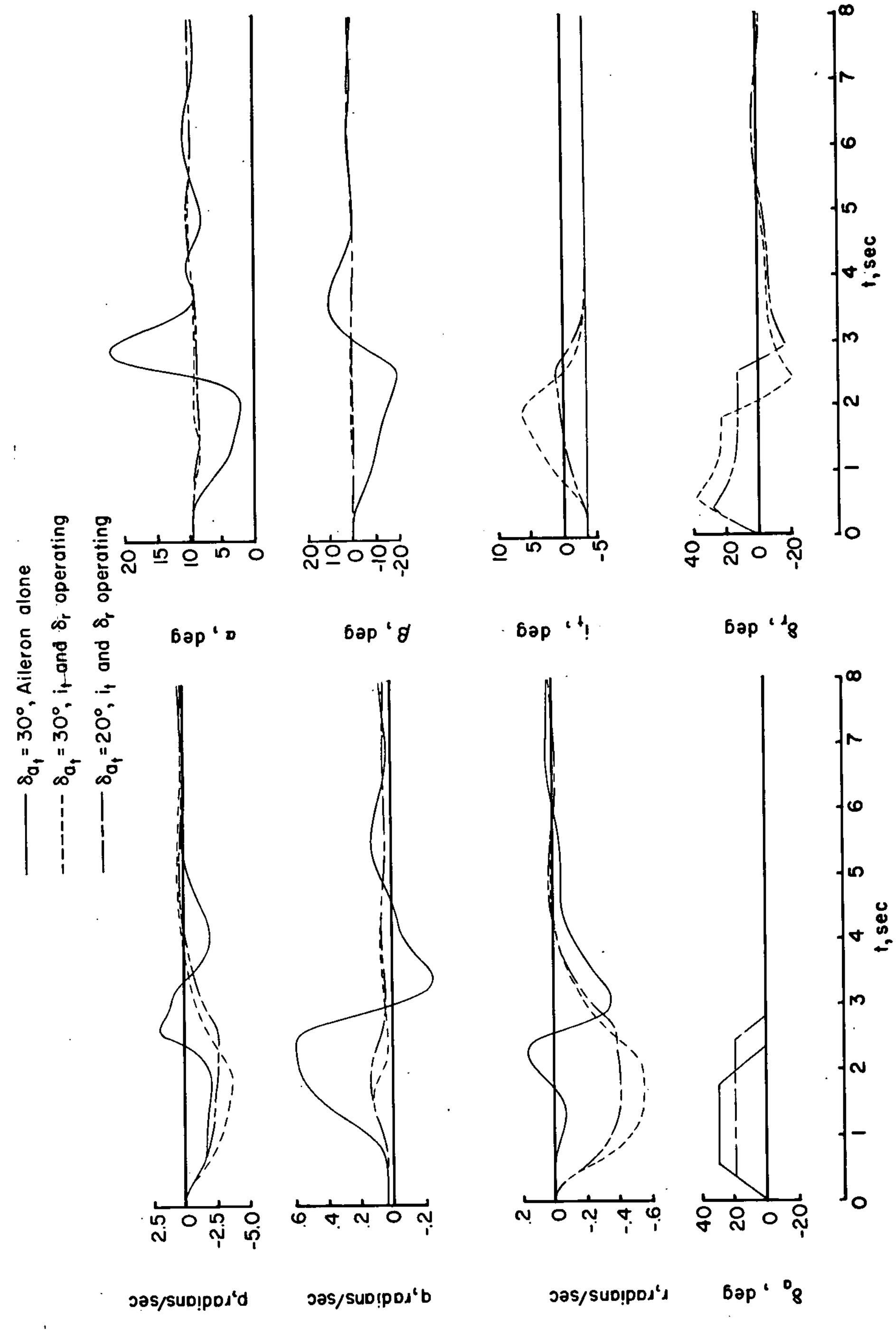

(c) $(n_g)_o = 2.$

Figure 5.- Concluded.

NACA - Langley Field, Va.